JOURNAL OF MORPHOLOGY 277:204–230 (2016)

Postcranial Osteogenesis of the Helmeted Water Toad *Calyptocephalella gayi* (Neobatrachia: Calyptocephalellidae) With Comments on the Osteology of Australobatrachians

Paula Muzzopappa,[1,2]* L. Analía Pugener,[3] and Ana María Báez[1,2,4]

[1]*Sección Paleontología de Vertebrados, Museo Argentino de Ciencias Naturales "Bernardino Rivadavia," Av. Ángel Gallardo 470, C1405DJR, Ciudad Autónoma de Buenos Aires, Argentina*
[2]*CONICET, Av. Rivadavia 1917 (C1033AAJ) Ciudad Autónoma de Buenos Aires, Argentina*
[3]*Facultad de Ciencias Exactas y Naturales, Universidad Nacional de La Pampa, Uruguay 151, CP 6300, Santa Rosa, La Pampa, Argentina*
[4]*Departamento de Ciencias Geológicas, Facultad de Ciencias Exactas y Naturales, Laboratorio de Paleontología Evolutiva de Vertebrados, Universidad de Buenos Aires, Intendente Güiraldes 2160, C1428EGA, Ciudad Autónoma de Buenos Aires, Argentina*

ABSTRACT *Calyptocephalella gayi* is one of over 6,000 neobatrachians arranged into two main groups, Hyloides and Ranoides. Phylogenetically, *C. gayi* is placed in Australobatrachia, a Gondwanan clade that is either the most basal clade of Hyloides or the sister group of Hyloidea, depending on the cladistic hypothesis; as such, this species is a key taxon in the study of the early evolution of Neobatrachia. The ontogeny of the postcranial skeleton of *C. gayi* is described in this article. The description is based on pattern of chondrification and ossification of skeletal elements in a growth series of tadpoles, on juveniles and adult individuals. Particular attention was devoted to some developmental aspects and morphological traits of the adult skeleton. The body of Presacral Vertebra VIII is formed from three centers of ossification, in contrast to the usual two dorsolateral centers observed in the remaining vertebrae of *C. gayi*, as well as in most anuran taxa for which the development of the axial skeleton is known. Each half of the pelvic girdle arises from a single cartilaginous element. The early development of the autopodia of both the forelimb and hindlimb includes the presence of an additional chondral element, which occurs during the formation of Distal Carpal 5 and the transient formation of Distal Tarsal 4 before the latter is incorporated in the cartilaginous distal end of the fibular. Some osteological aspects of other australobatrachian anurans also are reviewed (e.g., presence of intervertebral discs) based on reports in the literature, as well as first hand observations. In the course of this study, it became evident that further osteological studies are needed to formulate a clear picture of the evolution of skeletal characters not only within Australobatrachia, but also within Neobatrachia. J. Morphol. 277:204–230, 2016. © 2015 Wiley Periodicals, Inc.

KEY WORDS: Anura; Rana Grande Chilena; ontogeny; intervertebral discs; vertebral body ossification

INTRODUCTION

The aquatic helmeted frog, *Calyptocephalella gayi*, has attracted the attention of herpetologists since its description by Duméril and Bibron (1841). It is endemic to the moist Temperate Forest of Chile, where it is a conspicuous inhabitant of swamps, lakes, ponds, and quiet streams west of the Andes from the Coquimbo region (29°57′00″S) to Puerto Montt (41°28′00″S) (Krieg, 1924; Cei, 1962; Rabanal and Nuñez, 2008). Krieg (1924) provided the only known report on some aspects of the frog's natural history; the presence of tadpoles belonging to widely different developmental stages in autumn (May) led him to suggest that the larval development might take 1 or 2 years. The external features of larvae and adults have been described by several authors (e.g., Duméril and Bibron, 1841; Nieden, 1923; Krieg, 1924; Cei, 1962; Díaz and Valencia, 1985; Lavilla, 1988); in addition, there are anatomical studies of early organogenesis of the larvae (Jorquera and

Additional supporting information may be found in the online version of this article.

Contract grant sponsor: Agencia Nacional Ciencia y Tecnología; Contract grant number: (PICT 1895/11).

*Correspondence to: Paula Muzzopappa; Av. Ángel Gallardo 470, C1405DJR, Ciudad Autónoma de Buenos Aires, Argentina. E-mail: pmuzzopappa@gmail.com

Author Contributions: PM Collected, prepared, and studied the material. PM and LAP interpreted the results. PM, LAP, and AMB discussed the results and wrote the article.

Received 18 July 2015; Revised 22 September 2015; Accepted 24 October 2015.

Published online 23 November 2015 in Wiley Online Library (wileyonlinelibrary.com). DOI 10.1002/jmor.20490

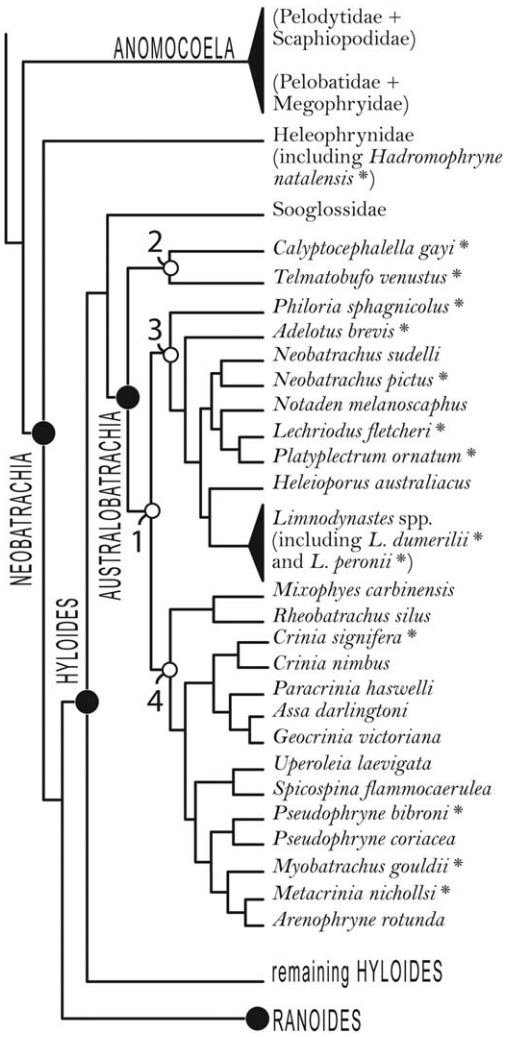

Fig. 1. Simplified phylogenetic hypothesis of Australobatrachia based on Frost et al. (2006). Node 1: Myobatrachoidea; Node 2: Calyptocephalellidae; Node 3: Limnodynastidae; Node 4: Myobatrachidae. The asterisk (*) indicates the species included in the analysis by Frost et al. that were examined in the present study. Frost et al. (2006) reffered to *Calyptocephalella gayi* as *Caudiverbera caudiverbera*.

Izquierdo, 1964; Jorquera and Pugin, 1975) and the skin histology of the adult (Moreno et al., 1978). However, few studies have dealt with the skeletal anatomy, the most important publications on this topic being those of Parker (1881) and Reinbach (1939) that focused on the skull of larvae and adults. Decades later, Reig (1960) briefly described the postcranial skeleton and Lynch (1971, 1978) provided some anatomical information on this species in his studies on the relationships of the former "leptodactylid" frogs.

In the last decade, several broad-scale phylogenetic analyses based on molecular and combined molecular and morphological data sets have been performed. In the few studies in which *C. gayi* was part of the taxon sampling, it was retrieved as a member of an early diverging neobatrachian clade, named Australobatrachia by Frost et al. (2006; *C. gayi* was named *Caudiverbera caudiverbera* in that paper) (Fig. 1). The clade also includes the Australopapuan Myobatrachoidea (= Myobatrachidae + Limnodynastidae) (San Mauro et al., 2005; Frost et al., 2006; Van der Meijden et al., 2007; Pyron and Wiens, 2011), which is the sister group of Calyptocephalellidae (i.e., *Calyptocephalella* and its sister taxon, the Chilean *Telmatobufo*, sensu Frost, 2015). The phylogenetic position of *C. gayi* has significant biogeographic implications and also imparts a key role to this taxon in informing our understanding of the early cladogenesis of Neobatrachia. Currently, no morphological characters support this evolutionary hypothesis (Frost et al., 2006: 193) in part because little is known about australobatrachid anatomy. In addition, the inter-relationships within Myobatrachoidea have not been unambiguously resolved (Frost et al. 2006; Pyron and Wiens, 2011), thereby limiting the interpretation of available data.

Herein we describe the adult features and skeletogenesis of the postcranial skeleton of *C. gayi*, providing an initial insight into this interesting clade, Australobatrachia, in the context of its phylogenetic position. As with the osteology, little is known on the development of members of Myobatrachoidea (Davies, 1989) and *Telmatobufo* (Fabrezi, 1992). This precludes detailed comparisons of the skeleton and development of *C. gayi* with those of its closest relatives.

MATERIALS AND METHODS

Most specimens of the developmental series examined were obtained in March 2007 in Pucón, Chile, from a frog farm authorized by the SAG (Servicio Agrícola Ganadero, Ministerio de Agricultura, Gobierno de Chile). There, they grew in natural ponds under wild conditions (i.e., intensive indoor frog culture techniques, such as larval rearing, were not applied in this farm). Once captured, anurans were euthanized with sodium pentobarbital (60–100 mg/kg of body weight) administered intrapleuroperitoneally in adults; larvae were euthanized in 4% formaldehyde (previously neutralized with disodium phosphate). Adults and larvae were fixed in 4% formaldehyde; adults were transferred to 70% alcohol and larvae to a fresh solution of 4% formaldehyde for storage.

Measurements were obtained with 0.02 mm-error calipers. Larvae were staged according to Gosner (1960); because the staging table for *C. gayi* by Jorquera and Izquierdo (1964) includes only the earliest stages of development, it could not be used in this study. Specimens MACN 39901.ej1 (approximately Stage 41) and MACN 39901.ej2 (approximately Stage 43) were staged according to the degree of development and erosion of cranial osseous and cartilaginous elements, respectively. Specimens are housed in the Museo Argentino de Ciencias Naturales "Bernardino Rivadavia," División Herpetología. Specimens were collected and euthanized according to the regulations specified by the Institutional Animal Care and Use Committee of the Facultad de Ciencias Exactas y Naturales, Universidad de Buenos Aires (Res C/D 140/00). The specimens examined are listed in Table 1.

TABLE 1. Examined material

Taxon	Collection number and description of specimen
Adelotus brevis (Günther, 1863)	KU 56242, M (Male), DS (Dry Skeleton); KU 147213, F (Female), DS; KU 179912, M, SVL 39.3 mm, c&s; KU 186773, M, DS; KU 186774, M, SVL 23 mm, DS.
Calyptocephalella gayi (Duméril and Bibron, 1841)	MACN 39894, 4 specimens, GS 34, c&s; MACN 39895, 5 spcm (specimens), GS 35, c&s; MACN 39896, 4 spcm, GS 36, c&s; MACN 39897, 3 spcm, GS 37, c&s; MACN 39898, 4 spcm, GS 38, c&s; MACN 39899, 1 spcm, GS 39, c&s; MACN 39900, 1 spcm, GS 40, c&s; MACN 39901, 2 spcm, GS 41 (ej1) and GS 43 (ej2), c&s; MACN 45741, M, SVL 100.1 mm, c&s; MACN 45742, F, SVL 112.4 mm, c&s; MACN 45743, M, SVL 100.5 mm, c&s and DS; MACN 45744, F, SVL 122.1 mm, c&s and DS; MACN 45745, F, SVL 162.4 mm, c&s and DS; MACN 45746, F, SVL 162.8 mm, c&s and DS; MACN 45747, F, SVL 154.1 mm, c&s and DS; MACN 45748, M, 140.9 mm, c&s and DS; MACN 45749, c&s and preserved in ROH 70%; MACN 45750, F, SVL 56.2 mm, c&s; MACN 45751, DS.
Crinia bilingua (Martin, Tyler, and Davies, 1980)	KU 180030, M, SVL 20.0 mm, c&s.
Crinia parinsignifera (Main, 1957)	KU 56248, c&s; KU 56249, c&s.
Crinia signifera (Girard, 1853)	KU 56243, M, c&s; KU 56244, M, c&s; KU 56245, F, c&s; KU 56246, M, c&s; KU 56247, F, c&s; KU 56348, F, c&s; KU 56349, F, c&s; KU 56364, F, c&s; KU 186775, DS.
Hadromophryne natalensis (Hewitt, 1913)	KU 195926, c&s.
Limnodynastes dumerilii (Peters, 1863)	KU 93553, F, DS; KU 186779, DS.
Limnodynastes fletcheri (Boulenger, 1888)	KU 93559, c&s; KU 186780, DS.
Limnodynastes peronii (Duméril and Bibron, 1841)	KU 93566, F, c&s.
Limnodynastes tasmaniensis (Günther, 1858b)	KU 93573, F, c&s; KU 93574, F, c&s
Metacrinia nichollsi (Harrison, 1927)	KUH 110332, c&s; KU 186781, F, DS.
Mixophyes fasciolatus (Günther, 1864)	KU 56627, F, DS; KU 147227, DS.
Myobatrachus gouldii (Gray, 1841)	KU 110333, c&s.
Neobatrachus aquilonius (Tyler, Davies, and Martin, 1981)	KU 93578, F, DS.
Neobatrachus pictus (Peters, 1863	KU 69278, M, c&s; KU 186777, F, DS.
Notaden nichollsi (Parker, 1940)	KU 93580, c&s; KU 93581, M, SVL 45.6 mm, c&s; KU 93582, c&s.
Philoria frosti (Spencer, 1901)	KU 50699, c&s; KU 186782, DS.
Philoria sphagnicolus (Moore, 1958)	KU 110331, c&s.
Platyplectrum ornatum (Gray, 1842)	KU 179936, F, SVL 33.2 mm, c&s; MACN 42620.
Pseudophryne bibronii (Günther, 1858a)	KU 93588, M, c&s; KU 93587, F, SVL 26.0 mm, c&s.
Pseudophryne semimarmorata (Lucas, 1892)	KU 186783, DS; KU 186784, DS.
Taudactylus acutirostris (Andersson, 1916)	KU 124233, F, c&s.
Telmatobufo venustus (Philippi, 1899)	KU 159811, DS; KU 161439, F, SVL 87 mm, DS.
Uperoleia fusca (Davies, McDonald, and Corben, 1986)	KU 180028, M, SVL 19.6 mm, c&s; KUH 205027, c&s.
Uperoleia rugosa (Andersson, 1916)	KU 109861, F, c&s; KU 186785, DS.
Uperoleia russelli (Loveridge, 1933)	KU 125355, M, c&s.

Institutional Abbreviations

CPBA-V—Departamento de Ciencias Geológicas, Paleontología, Vertebrados, Universidad de Buenos Aires, Ciudad Autónoma de Buenos Aires, Argentina; KU—The University of Kansas, Lawrence, Kansas; MACN—Museo Argentino de Ciencias Naturales "Bernardino Rivadavia," División Herpetología, Ciudad Autónoma de Buenos Aires, Argentina.

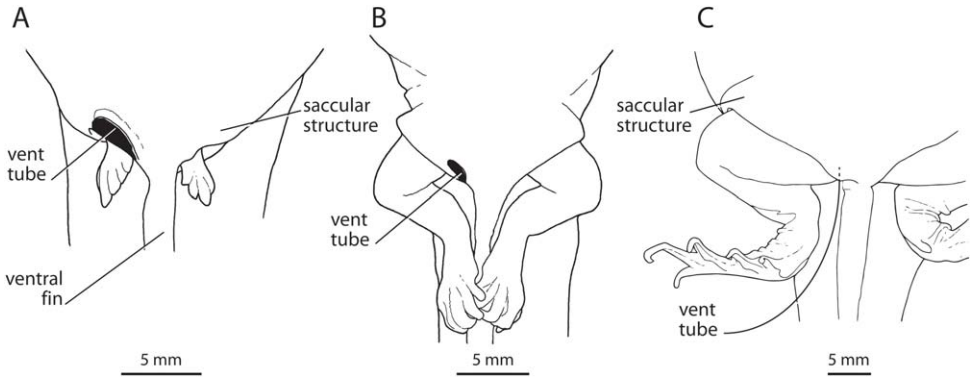

Fig. 2. *Calyptocephalella gayi*. Detail of the posterior portion of the abdomen at different larval developmental stages. (**A**) Stage 36. (**B**) Stage 39. (**C**) Stage 40. Note that at early stages a saccular structure (i.e., a fold of the body wall) completely envelops the hind limbs when retracted. At later stages, the limbs no longer fit in the fold.

Cartilage and Bone Staining. Dry Skeletons

Larvae and some adult specimens (see Table 1) were cleared and double-stained using the protocol of Taylor and Van Dyke (1985) modified as follows 1) larvae transferred to the Alcian Blue solution directly from formaldehyde and 2) enzymatic solution exposed to sunlight. These modifications significantly reduced the time to complete the treatment and also produced a more transparent musculature. Some adult specimens were dried (except for the pectoral girdle, forearm, hyoid, and laryngeal skeletons, which were cleared and double-stained) following the methodology of Simmons (1986), using a bleach to water ratio of 1:4 for several minutes to a few hours (depending on the part of the skeleton) and finally neutralizing the bleach with 96% ethanol for 15 min.

Histological, Anatomical, and Taxonomic Nomenclature

Because of the different use of some histological terms and to avoid confusion, we define the histological terms used herein. Those bones that have a cartilaginous precursor are enchondral (sensu Roček, 2003); they include endochondral and perichondral ossifications (sensu Castanet et al., 2003; Witten and Huysseune, 2007). In contrast, the terms dermal or membranous ossification often are used synonymously (e.g., Roček, 2003; Castanet et al., 2003) and refer to bones that are not preformed in cartilage.

Morphological nomenclature follows that of Lynch (1971), unless otherwise stated. In particular, the vertebral nomenclature follows that of Pugener and Maglia (2009) and the carpal nomenclature follows that of Fabrezi (1992). We follow the taxonomic framework of Frost et al. (2006), in which *C. gayi* (*as Caudiverbera caudiverbera*) is a member of the Calyptocephalellidae (originally Batrachophrynidae, but later renamed; Frost, 2015) and the latter, the sister group of Myobatrachoidea (= Myobatrachidae + Limnodynastidae); in turn, Calyptocephalellidae and Myobatrachoidea compose Australobatrachia, a basal clade within neobatrachian Hyloides. Pyron and Wiens (2011) obtained the same general topology, although the phylogenetic schemes differ in the internal relationships of Myobatrachidae and Limnodynastidae.

Illustrations were prepared with the aid of a Zeiss Stemi SV and Keerbrug Wild type 308700 stereo microscopes with camera lucida. The figures were prepared using Adobe Photoshop and Adobe Illustrator.

Anatomical Abbreviations

DC: Distal carpal. DT: Distal tarsal. MtC: Metacarpal. MtT: Metatarsal. NA: Neural arch. PV: Presacral vertebra. TP: Transverse process.

RESULTS

Observations on Larval External Morphology

We collected specimens of a wide array of developmental stages in the early autumn (end of March 2007), thereby supporting the hypothesis that the larval period may last 1 year or more (Krieg, 1924). In life, the tadpoles were observed to retract their hind limbs into a saccular structure located at the posterior end of the abdomen. The structure consists of a fold of the body wall that covers the vent tube and wraps the hind limbs, leaving a posterior opening through which limbs emerge. As the larvae develop, their limbs are further exposed until they no longer fit within the fold (Fig. 2). The presence of a similar structure has been reported for a few anuran taxa (e.g., the leiopelmatid *Ascaphus truei*, Stephenson, 1951; the hylid *Hyloscirtus*, Lötters et al., 2005 and Sánchez, 2010). A saccular structure inside which the hind limbs develop and resembling that of *C. gayi* was observed in Telmatobufo larvae (pers. obs.) and described for the larvae of the myobatrachid genus *Mixophyes* (Gradwell, 1975; Anstis, 2013).

Adult Postcranial Skeleton

The axial skeleton of *C. gayi* consists of eight procelous, presacral vertebrae (PVs I–VIII), one sacral vertebra (IX), and the urostyle (Fig. 3). The vertebrae are nonimbricate; however, the atlas has a high and robust neural spine that partially roofs the space between the neural arches of PV I and PV II. The atlas has two kidney-shaped cotyles that are narrowly separated medially (Type II of Lynch, 1971; Fig. 3C), a feature that persists even in the oldest specimens examined (MACN 45746 and MACN 45747). The atlantal cotyles form the ventral margin and half of the lateral margins of the neural canal. In dorsal view, the neural arches are quadrangular with extensive zygapophyses. The neural laminae of PVs IV and V are the largest of the vertebral series, whereas the sizes of the

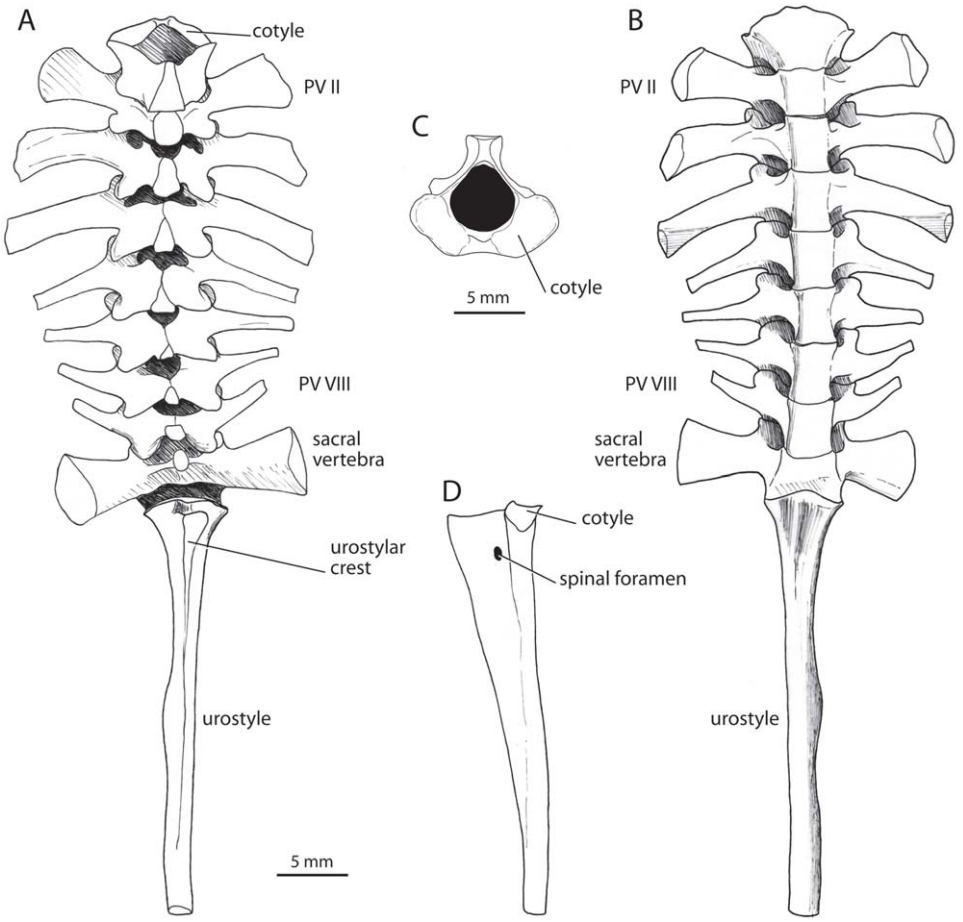

Fig. 3. *Calyptocephalella gayi*. Axial skeleton; drawings based on dry skeletons lacking the cartilaginous distal ends of the transverse processes. Vertebral column in (**A**) dorsal and (**B**) ventral views (MACN 45743). (**C**) Atlas in anterior view (CPBA-V 1533). (**D**) Urostyle in lateral view (MACN 45743). Abbreviation: PV = Presacral Vertebra.

other neural laminae decrease from that point both anteriorly and posteriorly. The neural spines of Vertebrae II–IX are posteriorly directed, but none extends beyond the level of the postzygapophyses. In the oldest individuals examined, the well-ossified neural arches almost completely cover the intervertebral spaces and the neural spines of the entire vertebral column are relatively uniform in height. The TPs of PV II–IV are the largest of the series. Those of PV II are the stoutest and widest, being as wide as the pedicle proximally and wider than it distally. The TPs of PV III have a marked ventral orientation, and are wide and distally expanded; their posterior margins bear uncinate processes. The TPs of PV IV are posteriorly and ventrally oriented. The distal ends of TPs of PVs III and IV bear cartilaginous hook-like expansions that extend posteriorly. PVs V–VIII bear acuminate, relatively long transverse processes that decrease in length posteriorly. The sacral diapophyses are markedly dorsally and posteriorly oriented; their anterior margins are perpendicular to the longitudinal axis of the vertebral column, whereas the posterior margins form an angle of about 30° with the same axis. The relative lengths of TPs are the same either considering their distal cartilaginous tips or considering only the ossified portion: IV $\approx$ III > II $\approx$ IX > V $\geq$ VI > VII $\approx$ VIII. The sacrum bears two subcircular condyles, separated by a deep notch, for the articulation with the urostyle. The urostyle is as long as the presacral region of the vertebral column and it has neither prezygapophyses nor transverse processes. A crest extends along the anterior three quarters of the dorsal surface of the urostyle; the crest is highest anteriorly and diminishes in height posteriorly. A foramen occurs on each side of its anterior portion. The two cotyles are oval to circular, separated by a shallow notch.

None of the PVs are fused with one another; however, partial fusions of vertebral centra (not including neural arches) occur either between PVs I and II (MACN 45745) or between PV VIII and the sacral vertebra (MACN 45744 and MACN 45747). Reig (1960) also noted an incipient fusion between PVs I and II. Asymmetrical sacralization

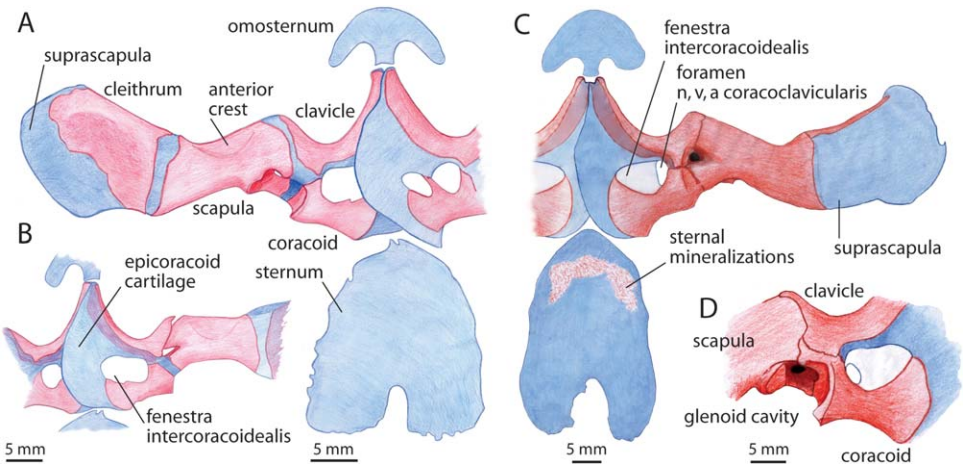

Fig. 4. *Calyptocephalella gayi*. Pectoral girdle. Right pectoral girdle of an adult individual in (**A**) glenoidal and (**B**) dorsal views (MACN 45741). Right pectoral girdle of an old individual in (**C**) dorsal and (**D**) glenoidal views (MACN 45745). Note the presence of cartilage between the coracoid and the *pars glenoidalis* and between the coracoid and the clavicle. In older specimens, these cartilages are ossified and the three elements are in tight contact. Blue denotes cartilage, red denotes bone. Abbreviations: n = nerve; v = vein; a = artery.

of PV VIII occasionally occurs; for example, in MACN 45745 and an unnumbered CPBA-V specimen, the sacral diapophysis is present only on the left side. Marelli (1927) also reported a similar situation that involved the sacral vertebra and the urostyle, both of which bore a sacral diapophysis. Neither the vertebral centra nor the neural spines have ornamentations or foramina, but in some of the oldest specimens the neural spines and the margins of the TPs are rugose. The vertebral centra are protuberant in ventral aspect; those of PVs IV–VIII are round in cross-section and relatively small compared with the total size of the vertebra, whereas the remaining centra are slightly depressed dorsoventrally.

The pectoral girdle (Fig. 4) is arciferal; the epicoracoid cartilages overlap broadly and are fused at their most anterior portion. The *fenestra intercoracoidealis* (sensu Havelková and Roček, 2006) or coracoid fenestra (fide Baleeva, 2009) (i.e., the space framed by the epicoracoid cartilage, the procoracoid cartilage, and the coracoid) is filled with a membrane pierced by one or two foramina; these vary in position in different individuals and they may correspond to the foramen which the coracoclavicularis nerve, artery, and vein (fide Gaupp, 1896) traverse. The large cartilaginous omosternum is fungiform in shape and bears a semilunar, flat anterior extension, the lateral ends of which project posteriorly. The maximum width of the omosternum matches the mediolateral length of the coracoids; despite the large size of the element, it is neither mineralized nor ossified in any specimen. The sternum is also large; its anteroposterior length is equivalent to that of the omosternum plus the epicoracoid cartilages. The sternum has an irregular margin and a deep posterior notch. Paired mineralizations, which may unite at the midline, occur in the largest specimens (MACN 45745, MACN 45746, and MACN 45747). The clavicles are robust and deeply curved anteriorly. Each element covers the anterior edge of the procoracoid cartilage, extending partially over the dorsal and ventral surfaces of the cartilage; the ventral part of the clavicle covers more of the procoracoid cartilage than does the dorsal part. In aged individuals (e.g., MACN 45746), the medial end of the procoracoids overlap. The lateral end of the clavicle articulates with the medial margin of the scapular *pars acromialis*. The coracoid is robust; its medial end is flat and asymmetrically expanded with the anteromedial part being more expanded than the posteromedial part. The maximum anteroposterior expansion of the medial end of the coracoid is equivalent to 80–90% of the maximum overall length of the bone. The glenoidal (lateral) end of the coracoid is oval to quadrangular in cross section; it is in contact with the clavicle anteriorly and the scapular *pars glenoidalis* laterally, thereby forming part of the glenoid cavity. In young adults, there is cartilage between the lateral end of the coracoid and the *pars glenoidalis*, as well as between the former bone and the clavicle. In older specimens, these cartilages are ossified and the three elements are in tight contact (Fig. 4D). In one of the specimens examined (MACN 45741, Fig. 4A,B), the leading edge of the coracoid has an anterior projection (especially evident on the left side) that extends into the *fenestra intercoracoidealis*. The scapula is robust: it is trapezoidal and wider than long. The maximum mediolateral length is about 110% that of the coracoid (contra Reig, 1960, who described the scapular length as being more than twice that of the

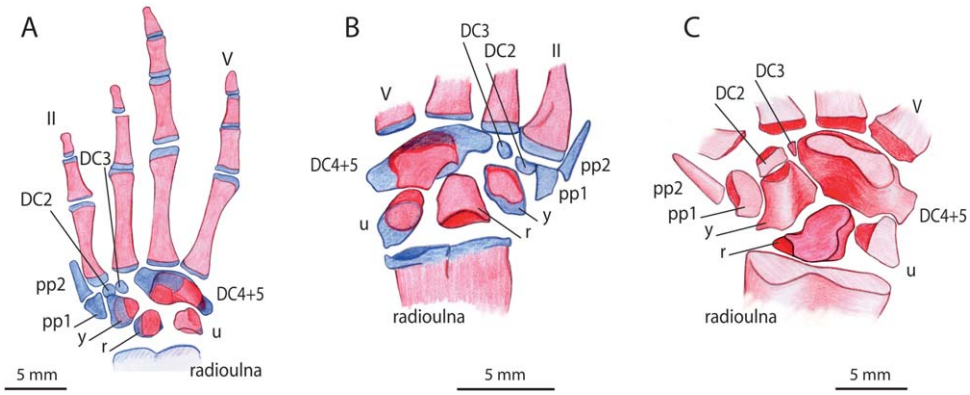

Fig. 5. *Calyptocephalella gayi*. Manus. Right manus (**A**) in dorsal view and (**B**) detail of the carpus in palmar view (MACN 45741). (**C**) Left manus of an old individual showing a detail of the carpus in palmar view (MACN 45745). Note the differences in the degree of ossification of the distal carpals and prepollical elements. Blue denotes cartilage, red denotes bone. Abbreviations: II = Digit II; V = Digit V; DC = Distal Carpal; pp = prepollical element; r = radiale; u = ulnare; y = Element Y.

coracoid). The medial end is bicapitate and the anterior margin bears a conspicuous anterior crest (*tenuitas cristaeformis* of Bolkay, 1919) that extends from the medial end to near the lateral end of the bone. The *pars acromialis* is more extensive than the *pars glenoidalis*. Laterally, the scapula is continuous with the ample suprascapular cartilage. The cleithrum and the scapula are separated by a strip of suprascapular cartilage; however, in the older, more-ossified individuals, these elements are in contact. The suprascapular cartilage is equal in size or even larger than the scapula; distally, it is expanded and convex. The cleithrum is uniramous and invests approximately 50–75% of the dorsal surface of the suprascapular cartilage, extending along its proximal and leading edges.

The forelimb is well ossified. The humerus is robust; the distal end is sharply curved laterally. The proximal end is completely ossified in the largest specimens. On the ventral surface of the diaphysis there is a high deltoid (or ventral) crest, the distal half of which diminishes abruptly in size. Another crest projects on the medial side of the deltoid crest, forming a groove with the latter for the tendon of the *m. coracoradialis*. The distal end of the humerus is configured into two prominent, similarly developed ulnar (or medial) and lateral epicondyles that flank a well-ossified humeral ball. The diameter of the ball constitutes more than 50% of the distal width of the humerus. The curvature of the humerus results in the ball being laterally displaced with respect to the long axis of the diaphysis. The radioulna bears a well-developed olecranean process proximally and its broad distal end is in contact with the basal elements of the autopodium. The carpus is composed of seven elements (Fig. 5). The radiale, a large Element Y, and two prepollical elements (pp1, pp2) compose the preaxial series. The prepollical distal element (pp2) is elongated and conical. The postaxial series comprises the ulnare, a large DC 4 + 5, a small DC 3 (the smallest of the carpal elements), and a small DC 2. In young adults, only the radiale, ulnare, Element Y, and a portion of the DC 4 + 5 are ossified (Fig. 5A,B), whereas all of the carpal elements are ossified in old individuals (Fig. 5C). The longest metacarpal is MtC IV, followed by MtC III, MtC V, and MtC II. The phalangeal formula is 2-2-3-3. Each of the conical terminal phalanges has a distal constriction that results in a rounded dilation at the apex.

The pelvic girdle (Fig. 6) is composed of two pairs of bones, the ilia, and ischia, along with the cartilaginous remnants of the puboisquiadic plates (*cartilago remanens* of Gaupp, 1896). When articulated, the ilia confer a V-shape to the pelvic girdle in dorsal view. Each ilium bears a high dorsal crest with a slight medial deflection that extends along the posterior two thirds of the shaft. A long dorsal protuberance occurs on a dorsal prominence confluent with the base of the crest. At the level of the articulation between the ilium and the sacral diapophysis, a cartilaginous ovoid sesamoid is present. The relative size of the ischium varies ontogenetically; overall, it is oval with a rounded posterior margin. The acetabulum is deep, not pierced at its bottom, and approximately circular; its dorsal margin has a small notch. A discrete ossified pubis was not discernable in any of the specimens examined. In some mature, well-ossified individuals, only a minimal strand of puboischiadic cartilage separates the ilium from the ischium in the ventral portion, or the bony elements articulate with one another therein.

The hind limb is approximately 50% longer than the forelimb. The femur and tibiofibula are about the same length, whereas the length of the proximal tarsals is more than one half the femur length. The femur bears a lateral crest that extends along the proximal half of the posterior aspect of the element (Fig. 6D). The proximal and

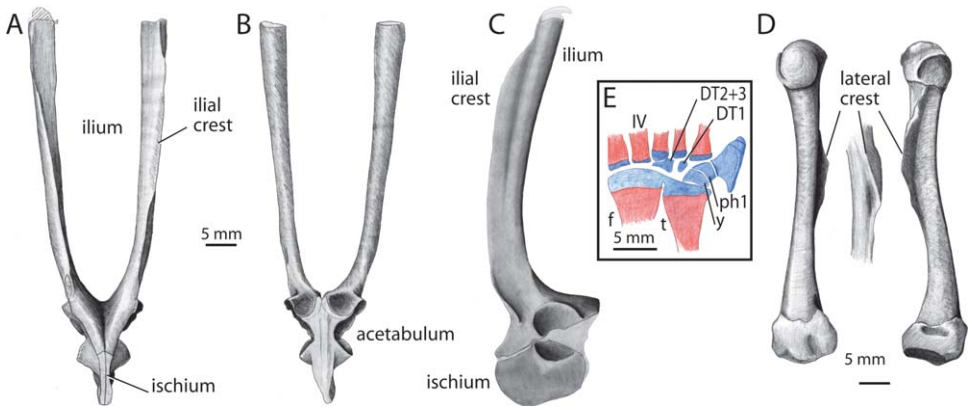

Fig. 6. *Calyptocephalella gayi*. Pelvic girdle, femur, and distal tarsus. Pelvic girdle in (**A**) dorsal, (**B**) ventral, and (**C**) lateral views (MACN 45743). Femur in (**D**) dorsal (left) and ventral (right) views and detail of lateral crest in lateral (center) view (MACN 45743). (**E**) Left tarsus in dorsal view (MACN 45742). Abbreviations: IV = Digit IV; DT = Distal Tarsal; ph = prehallical element; f = fibulare; t = tibiale; y = Element Y. In A–D, light gray denotes cartilage and dark gray denotes bone; in E, blue denotes cartilage and red denotes bone.

distal cartilaginous epiphyses of the tibiale and fibulare are fused. Distal to the latter bones, the tarsus is composed of a preaxial series comprising a conspicuous Element Y and a prehallux, and a postaxial series formed by a DT 2 + 3 and a DT 1 (Fig. 6E). The prehallux has a large basal element with a proximally directed spur and two or three distal elements of much smaller size. All tarsal elements (except the tibiale and fibulare) are cartilaginous in adults but mineralized in the most mature individuals. MtT IV is the longest, followed by MtTs V and III, MtT II, and MtT I—in order of decreasing size. The phalangeal formula is 2-2-3-4-3. The conical terminal phalanges have rugosities on the plantar surfaces of the distal tips.

Postcranial Development of *C. gayi*

The following description is organized by skeletal units (axial skeleton, pectoral girdle and forelimb, and pelvic girdle and hind limb). Each section includes a detailed description of the corresponding skeletal elements at Stage 34, the earliest stage examined, followed by an account of the main modifications of each element in subsequent stages. A synthesis of the osteogenesis is provided in Table 2.

Axial skeleton. In Stage 34, the axial skeleton is mostly cartilaginous (Fig. 7A). The NAs of Vertebrae I–IX, as well as the rudiments of NA X, are present as paired hemilaminae. Specimens MACN-HE 39894.ej1 and MACN-HE 39894.ej3 also have primordial NAs of two additional postsacral elements (XI and XII). A strip of loose cartilage unites the left and right hemilaminae of NAs I–IX, suggesting a recent fusion of the two halves. The NAs are short and separated from the adjacent arches by a distance equivalent to their anteroposterior length. The anterior margin of each NA is concave; this curvature becomes progressively more pronounced caudally, so that the anterior margins of NAs IV–IX are semicircular. The width of the NAs decreases posteriorly; hence, the width of NA IX is one half that of the atlas. The NA X is represented by two small, parallel strips of cartilage that are widely separated along the midline. The TPs of all of the PVs project laterally from the respective NAs; those on PVs II and III are 50% longer lateromedially than the corresponding NAs, whereas in PVs IV–VIII, they are represented only by conical primordia. Neither TPs nor zygapophyses are evident on the postsacral elements. The pedicles (the portions of NA that contact the vertebral centrum) of all vertebrae are cartilaginous. Ossification of the NAs has already started in Stage 34; thus, ossifications on the lateral portions of the neural laminae are visible at PVs I–VIII. Ossification is more extensive in the anterior vertebrae, where it invades the proximal halves of TPs of PV II and the proximal one thirds of TPs of PV III, but the zygapophyseal regions are unossified in all vertebrae.

Throughout ontogeny, ossification of the neural arches spreads medially and laterally, extending over the transverse processes. The zygapophyses, the middorsal portion, and especially the pedicles remain cartilaginous until early postmetamorphic juvenile stages. The TPs of the anterior PVs develop more rapidly than those of the posterior presacral and sacral vertebrae (Fig. 7A–F). The presacral NAs lengthen at Stage 36, resulting in reduced intervertebral spaces. In Stage 37, NAs I and II are closer to each other than previously, and those of PVs V–VIII are more quadrangular, resembling the adult morphology. The zygapophyses of the NAs widens at Stage 43; thus, the overlap between prezygapophyses and postzygapophyses is more extensive than in previous stages. The ossification of NA IX is first observed at Stage 35 as bilateral. The postsacral

*TABLE 2. Chondrification and ossification sequence of C. gayi**

Stage	Chondrification	Ossification
34	Neural Arches I–X (±Neural Arches XI, XII) Vertebral centra I–IX Hypochord Procoracoid Coracoid Scapula Suprascapula Humerus Radius Ulna Carpal elements: u, u', r, r', DC 5 +?, DC 4, DC 3, y, y' Metacarpals II–V Puboischiadic plate Femur Tibia Fibula Tibiale Fiulare DT 4, DT 2 + 3 Metatarsals II–V (±Metatarsal I)	Neural Arches I–VIII Vertebral Centra I–VI Cleirthum Humerus (±Scapula) (±Ulna) Femur Tibiafibula (±Ilial shaft)
35	Neural Arches XI, XII (present in all specimens) Epicoracoid complete DC 2, pp1 Tarsal Element Y, ph 1 Metatarsal I	Neural Arch X (±Neural Arch XI) (±Vertebral Centra VII, VIII) Additional ossification on Vertebral Centrum VIII Vertebral Centrum IX Clavicle (±Coracoid) (±Radius) Metacarpals IV, V
36	DT 1	Tibiale, Fibulare Metatarsals II–V
37	Neural Arch XIII pp2, Manus Phalangeal formula, complete	Metacarpals II, III Metatarsals I, II
38	pp3, ph2	Hypochord
39	ph3	
40	ph4	Ischium
Juvenil	Omosternum Sternum	r, u, y, DC 4 + 5 (partial)
Adult		Distal carpals, Prehallux

*Bones are listed by first Gosner Stage in which they appear.
Abbreviations: DC = Distal Carpal; DT = Distal Tarsal; ph = prehallical element; pp = prepollical element; r = radiale; u = ulnare; y = Element Y.

NAs are better developed in Stage 35 than in the previous stage, although they remain as paired structures dorsolateral to the neural tube. NA X is nearly completely ossified and is bridged by a strip of cartilage on each side of the vertebral column with NA XI; this bridge ultimately forms the margin of a spinal nerve foramen. The right and left halves of NA X are connected by a dorsal bridge of cartilage at their anterior margins in Stage 37 (MACN 39897.ej1 and MACN 39897.ej3); they change their relative positions at Stage 39, when they settle more dorsally, giving to the coccyx a triangular appearance in dorsal view. Posteriorly, NAs XI and XII remain as two elongate strips of cartilage at Stage 35 (NA XI ossified in MACN 39895.ej4). The ossification of NA XI is variable at Stage 37 (it is either completely ossified—MACN 39897.ej3—half ossified—MACN 39897.ej1—or entirely cartilaginous and poorly developed—MACN 39897.ej2), but present in all the specimens examined by Stage 38. NAs XII (MACN 39897.ej2, MACN 39897.ej3) and XIII (MACN 39897.ej1) are present as two pairs of longitudinal strips of cartilage at Stage 37, and they are connected by cartilaginous strings at either side of the vertebral column by Stage 38. The coccyx is formed by Stage 43 through fusion of the postsacral NAs formerly separated dorsomedially into right and left portions. On each side, there are two foramina—one large foramen between NAs X and XI and a smaller one (about one fourth the size of the former) in a more dorsal position between NAs XI and XII, but only one spinal foramen on each side remains after

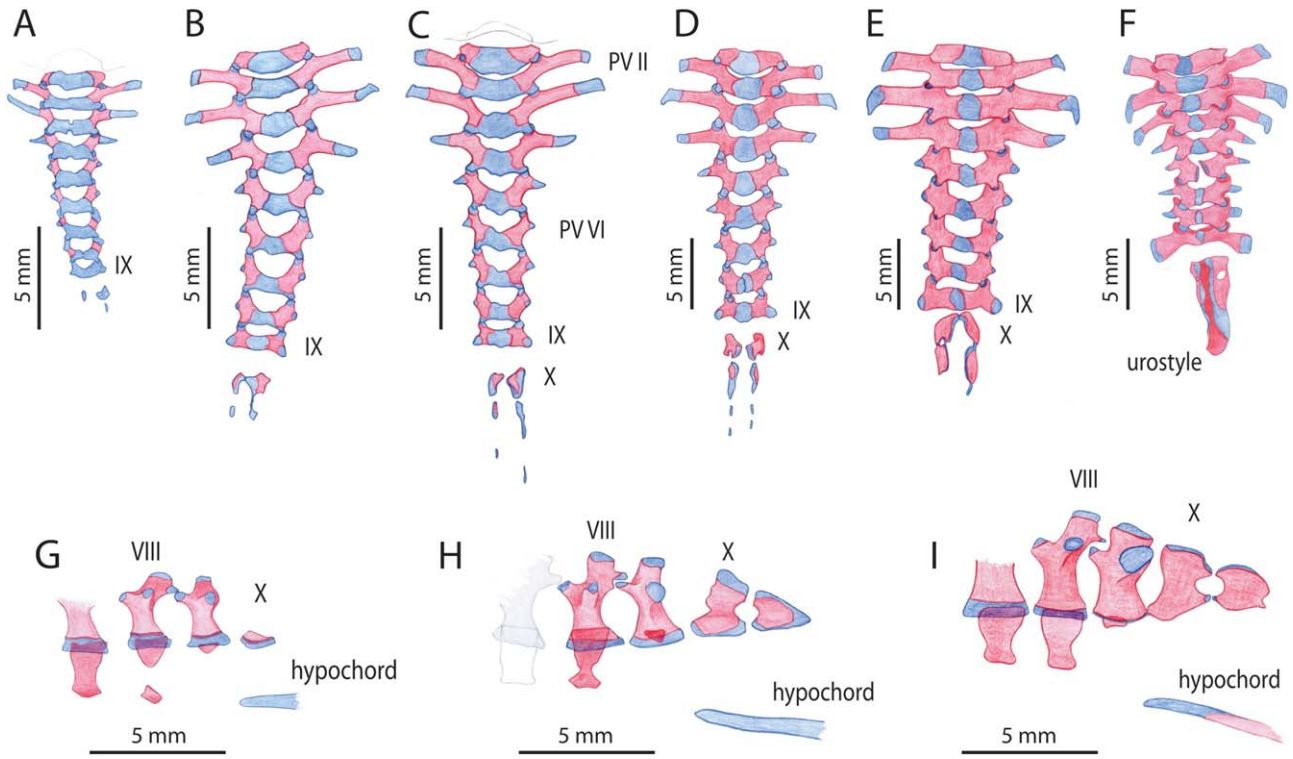

Fig. 7. *Calyptocephalella gayi*. Ontogeny of the axial skeleton. Dorsal view at (**A**) Stage 34 (MACN 39894.ej1), (**B**) Stage 35 (MACN 39895.ej2), (**C**) Stage 36 (MACN 39896.ej2), (**D**) Stage 37 (MACN 39897.ej2), (**E**) Stage 40 (MACN 39900), and (**F**) juvenile (MACN 57750). Lateral view at (**G**) Stage 37 (MACN 39897.ej1), (**H**) Stage 38 (MACN 39898.ej1), and (**I**) Stage 40 (MACN 39900). Note the additional center of ossification in Presacral Vertebra VIII. Abbreviations: VIII–X = number of posterior neural arches; PV = Presacral Vertebra. Blue denotes cartilage, red denotes bone.

metamorphosis. Postmetamorphic specimens lack ossified neural spines; instead, the middorsal portions of all neural arches, including the urostyle, are cartilaginous. The pedicles of the NAs have ossified, joining the NAs to the corresponding vertebral centra (Fig 8A–C). The atlantal cotyles are formed by the neural arches, the pedicles of which extend ventrally, wrapping the vertebral centrum.

The lengths of the TPs of PV III exceed those of PV II and the distal ends of the former TPs acquire cartilaginous hook-like processes that persist into adulthood from Stage 35 onward. TPs of PV II become larger than the corresponding NA and dilated at midlength to produce a spindle shape by Stage 41; at the same stage, the anterior–posterior widths of the TPs of PV III are greater than that of the corresponding NA. TPs of PV IV become robust and rectangular with blunt ends at Stage 37, but are acuminate, with an anteriorly curved cartilaginous distal end at Stage 41. In juveniles, the cartilaginous tips of TPs of PV IV are hook-shaped, resembling those of PV III. The TPs of PVs V–VIII resemble small domes at Stage 36, but are somewhat lengthened by Stage 40. The sacral diapophyses start to lengthen at Stage 39, although they are still short and robust by Stage 40. The ossification is extensive on the anterior PVs early in ontogeny; thus at Stage 36, those of PV II are almost completely ossified, while the proximal halves of PVs III and IV are ossified; their ossification is almost complete at Stage 37. On the contrary, the posterior PV (PVs V–VIII) remains mostly cartilaginous until the latest larval stages; ossification is restricted to their bases by Stage 40 but is extensive in postmetamorphic specimens. In contrast, the sacral diapophyses are already extensively ossified by Stage 40. The relative overall lengths of the TPs also change during ontogeny; they are III > II > IV > V ≥ IX > VI ≥ VII = VIII at Stage 35—but if only the ossified portion is considered, the order is II > III > IV > V—and it is III > II ≥ IV > V ≥ IX > VI > VII > VIII at Stage 39. Considering only the osseous partion—distal cartilages were not preserved—the relative lengths by Stage 41 are III > II > IV > IX > V > VI = VII = VIII and change to III > IV > II ≫ IX > V > VI = VII = VIII at Stage 43.

The vertebral centra form on the ventral side of the axial column and subsequently ossify from the perichordal cartilage that surrounds the notochord (Mookerjee, 1931). In Stage 34, this cartilage forms discrete perichordal arches that extend from the dorsolateral region to the middorsal and

midventral sides of the notochord. The arches are longest in PV I, where they are nearly in contact ventrally to form a cartilaginous ring; in contrast, they are shortest in Vertebrae VII–IX, where only the dorsolateral portions are present (in some cases without dorsomedial fusion of left and right halves). There are paired centers of ossification in each centrum dorsolateral to the notochord and deep in the perichordal arch (i.e., where the perichordal arch is in contact with the notochord—clearly evident in PV III of MACN 39894.ej1). The degree of ossification varies among the specimens examined. It is restricted to the most dorsal region of PVs I–III in the least ossified specimen (MACN 39894.ej1), but it already surrounds the notochord in PV I and PVs IV–VI, forming an osseous perichordal ring in the most ossified specimen (MACN 39894.ej4). Ventral to the notochord, a cartilaginous rod identified as the hypochord is visible below the NA X and the following four myotomes. The ventral surface of the hypochord is convex and its posterior end underlies a deep concavity on the ventral surface of the notochord (MACN 39894.ej1 and MACN 39894.ej3).

The ossification of the vertebral centra is restricted to the inner portion of the perichordal cartilage by Stage 35. It encircles the notochord forming osseous perichordal rings in PVs IV–VI in all of the specimens examined at Stage 35, thus being these the first centra to complete the perichordal ossification. PVs I and VII have an osseous perichordal ring in most specimens at Stage 35 and in all specimens at Stage 36. The osseous perichordal rings of PVs II and III are among the last to be formed; they may be either completely closed ventrally or have a small constriction at the midventral line—suggesting a recent fusion of both sides of the arch—by Stages 35–40 (MACN 39895.ej3; MACN 39897.ej1, MACN 39899, MACN 39900). The osseous perichordal rings are anteroposteriorly shorter than the pedicles of the corresponding NAs in Stage 35; noteworthy, that of PV I is twice as long as any other PV. The vertebral centra lengthen at Stage 39, reducing the intervertebral spaces, and are close to one another by Stages 41–43—closure decreases craniocaudally. At Stages 41–43, the perichordal rings of PVs IV–VII have a midventral posteriorly directed projection. The vertebral centrum of PV VIII has a cartilaginous arch that extends along the dorsal and dorsolateral portions of the perichordal arch and a small dorsal ossification in its inner portion at Stage 35. Furthermore, PV VIII has an additional ossification ventral to the notochord, which seems not to be related to the cartilaginous perichordal structure (Fig. 7G, see figures in Additional Supporting Information). This ossification appears in Stage 35 (MACN 39895.ej1), and is still evident by Stage 39, when a lateral constriction is evident on the frog's right side of the perichordal ring—at

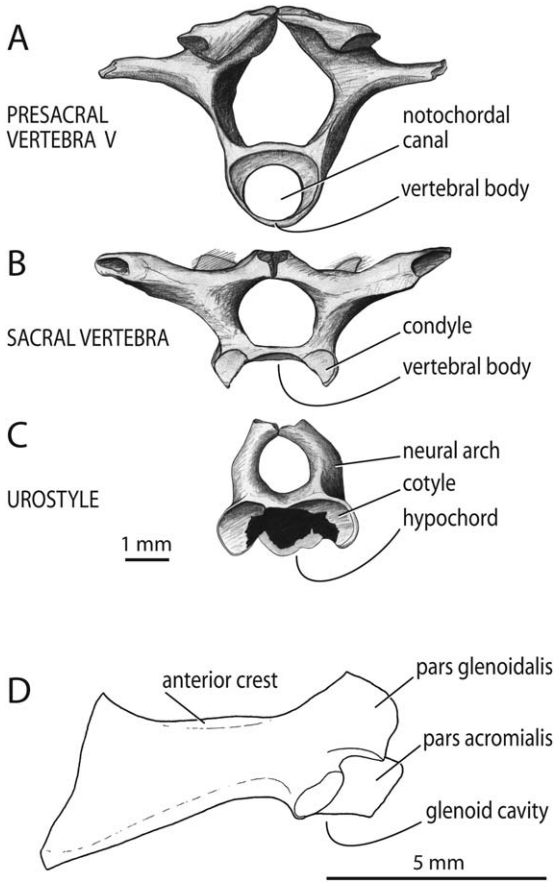

Fig. 8. *Calyptocephalella gayi*. Juvenile specimen (MACN 45751). Axial elements in anterior view: (**A**) Presacral Vertebra V, (**B**) sacral vertebra, and (**C**) urostyle. (**D**) Scapula in ventral view. Abbreviations: PV = Presacral Vertebra. Note the notochordal canal in PV V, the sacral condyles and urostylar cotyles (which form from the neural arches during the development of the sacrourostylar articulation), and the incipient anterior crest on the leading edge of the scapula.

Stage 37, either a dorsal perichordal arch separated from the ventral element (MACN 39897.ej2) or two lateral contrictions resulting from the fusion of these ossifications (MACN 39897.ej1) can be observed at the perichordal ring (Fig. 7G–I). The aforementioned morphology has been observed in PV VII, instead of PV VIII, in one specimen (MACN 39897.ej3). The presacral vertebral centra of postmetamorphic specimens have prominent notochordal canals (Fig. 8A); the perichordal ring is thick dorsally and much thinner ventrally in postmetamorphic specimens. The sacral vertebra is the least developed of the series. The perichordal arch is restricted dorsal to the notochord and lacks any evidence of ossification at Stage 35; by Stage 37, the ossification is weak, restricted to two separated ossification centers dorsolateral to the notochord; by Stage 40, the perichordal arch extends barely farther than the pedicles of the NA (Fig. 7I). In postmetamorphic specimens, the sacral centrum is still poorly

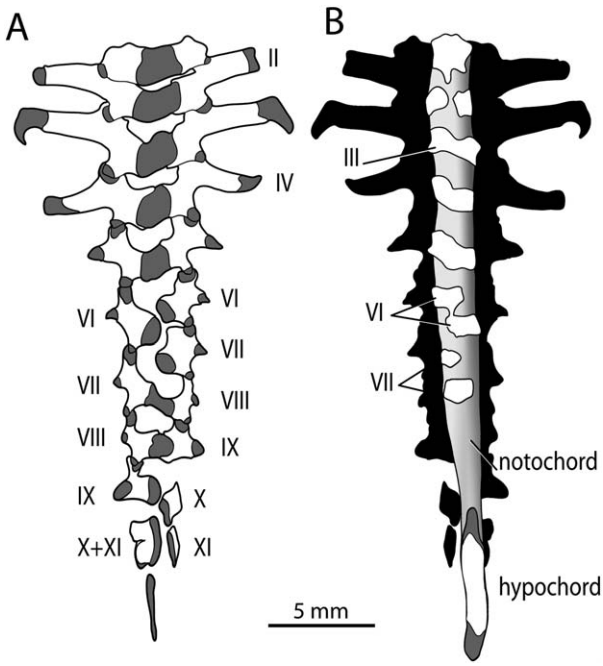

Fig. 9. *Calyptocephalella gayi*. Vertebral column of an abnormal specimen (MACN 39898.ej2) in (**A**) dorsal and (**B**) ventral views. Abbreviation: II–XI = number of axial elements. Dark gray denotes cartilage, white denotes bone, light gray denotes the notochord, and black represents the silhouette of the neural arches. Note the displacement of right and half sides of the axial elements.

ossified, restricted to the dorsal portion of the notochord and enclosed between the ossified pedicles of the NA. Despite the poor development of this vertebral centrum, one can observe the incipient formation of the condyles for the articulation with the urostyle; at least initially, they are formed from the NAs (Fig. 8B). Posterior to the vertebral series, the hypochord extends along five myotomes at Stage 37, but it is difficult to observe clearly at this stage. A center of ossification is first observed at midlenght of the cartilaginous hypochord by Stage 38, and it spreads to the entire element but the posterior portion by Stage 40. The hypochord is U-shaped in cross section, surrounding the ventral portion of the notochord by Stages 41–43. At Stage 40, the hypochord is well separated from the coccyx; it fuses to the ossified postsacral NAs in postmetamorphic specimens. In anterior view, the cotyles of the urostyle are clearly visible; they form from NA X (Fig. 8C).

It should be noted that no chondrification or ossification of postsacral vertebral centra were observed during development. Additionally, some abnormalities should be mentioned, such as the presence of rudimentary transverse process on the right side of the NA X in MACN 39895.ej4. Also, the right half of each vertebral element is displaced forward to the left half in MACN 39898.ej2. This displacement is especially marked posterior to PV V, where the halves of NA VI are separated from one another and in alternate positions with the right half of PV VII. The left half of NA VII is adjacent to the right half of NA VIII, with which it is fused, a pattern that is repeated posteriorly (Fig. 9A). Both sacral diapophyses develop from NA IX; the displacement of right and left NA of this element would have resulted in an adult specimen with an asymmetrical sacralization—the left sacral diapophysis would have been in Vertebra VIII and the right one, in Vertebra IX. The vertebral displacement is also evident in the vertebral centra. As with the dorsal elements, the displacement is more evident posterior to PV V. In PVs VI and VII, each of the ossification centers of the perichordal arch extends ventrally forming hemiperichordal arches that reach the ventral portion of the notochord (Fig. 9B).

Pectoral girdle and forelimb. In Stage 34, the pectoral girdle is composed of separate halves, each located at the posterolateral corner of the chondrocranium and formed by a continuous cartilaginous sheet in which the procoracoid, coracoid, scapular, and suprascapular cartilages can be discerned (Fig. 10A); however, the boundaries of these elements are not evident. Poorly organized cartilaginous tissue between the scapular and suprascapular cartilages, only visible at this stage, may correspond to the emerging cartilaginous bridge that unites the inferior and superior scapular cartilages, originating the scapula/suprascapula complex (Baleeva, 2001). The procoracoid and coracoid cartilages are poorly developed. The former is elongated lateromedially and bears a posteriorly directed hook on its medial end; this may represent the incipient development of the epicoracoid cartilage (Fig. 10B). The coracoid cartilage is subeliptical and half the length of the procoracoid cartilage. The funnel-shaped scapular cartilage is slightly shorter than the suprascapula. The *partes acromialis* and *glenoidalis* are apparent, circumscribing the glenoid foramen. The scapular cartilage has traces of perichondral ossification at midlength in MACN 39894.ej3 and MACN 39894.ej4. The subtriangular suprascapular cartilage overlaps the distal end of the corresponding transverse process of PV II. The cleithrum is present and well ossified in every specimen; it invests two thirds of the central portion of the anterior half of the suprascapular cartilage. The zeugo and stilopodia are approximately the same length (except in MACN 39894.ej3, in which the stilopodium is half the length of that of the zeugopodium). The radius and ulna are independent, well-chondrified elements (Fig. 11A). Incipient perichondral ossification is present in the diaphyses of the humerus and the ulna (except in MACN 39894.ej1, still cartilaginous). The carpus comprises nine isolated, cartilaginous condensations identified as ulnare, ulnare', radiale, radiale', DC

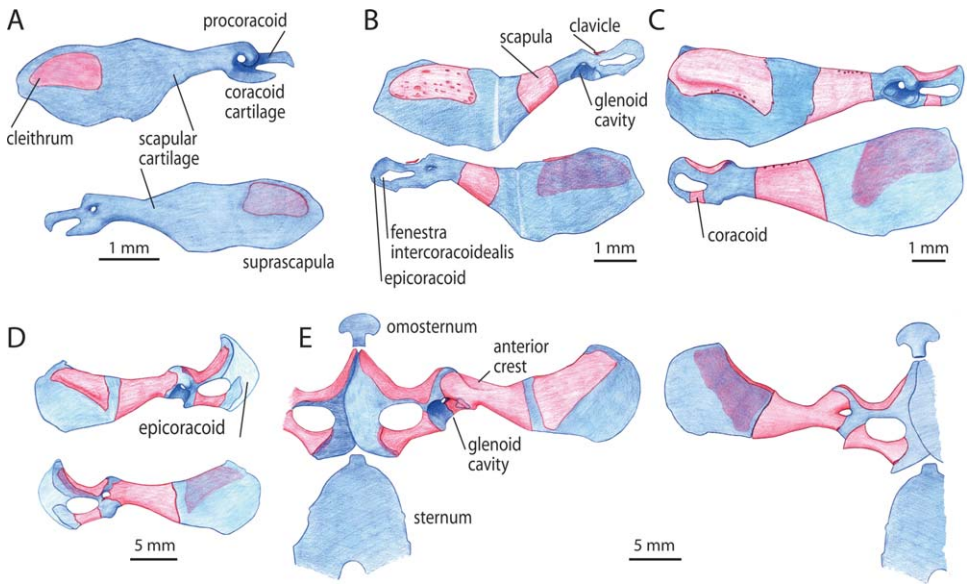

Fig. 10. *Calyptocephalella gayi*. Ontogeny of the pectoral girdle. Right half of the pectoral girdle in glenoidal (upper) and dorsal (lower) views at (**A**) Stage 34 (MACN 39894.ej1), (**B**) Stage 35 (MACN 39895.ej1), (**C**) Stage 37 (MACN 39897.ej1), and (**D**) Stage 43 (MACN 39901.ej2). (**E**) Right half of pectoral girdle of a juvenile in glenoidal (left) and dorsal (right) views—the sternum is incomplete (MACN 45741). Blue denotes cartilage, red denotes bone. Note the continuous cartilaginous sheet in which the procoracoid, coracoid, scapular and suprascapular cartilages are present in Stage 34. The cleithrum is already well ossified by Stage 34. The epicoracoid cartilage is completely developed at Stage 35, probably from the procoracoid. Sternal elements are present in juvenile individuals.

5 + ?, DC 4, DC 3, Element Y, and Element Y' (aligned, distal and preaxial to the radiale) (Fig. 11A). All the chondrifications are oval, but they differ in size. The configuration and size of DC 5 suggest that two cartilaginous condensations are involved in the formation of this element. There is a large one associated with the bases of MtCs IV and V, and a small one lateral to this; both condensations are immersed in the same cartilaginous nucleus. Distally, MtCs II–V and the first phalange of Digits III–V are present (Fig. 11A). In all specimens, MtC IV is the most developed, whereas MtC II is the least.

With respect to the overall structure of the pectoral girdle, the glenoid cavity is large and well formed by Stage 35 reflecting the development of its proximal and distal walls (*fovea acetabulum* and superficial articulation sensu Procter, 1921) formed by the coracoid and scapula, respectively. The glenoid cavity has an obvious ventral orientation in the early stages of development (Stages 34–36), but during later stages, it rotates; by Stage 37, the cavity has a slight posteroventral orientation, and by Stage 43, it faces more clearly posteroventrally. By Stage 40, the halves of the pectoral girdle are close to each other, but the epicoracoid cartilages do not overlap. The poor state of preservation of the available specimens precludes establishing the relative positions of these cartilages with respect to each other at later stages of metamorphosis.

The epicoracoid cartilage is completely developed by Stage 35 (Fig. 10B) and it increases in width at the level of the *fenestra intercoracoidealis* by Stage 40. The clavicle is present at Stage 35 and invests the anterior margin of the procoracoid cartilage (Fig. 10B); however, the degree of development varies individually. At its least development, the clavicle is a splint on one side (MACN 39895.ej5); subsequently, it increases in size to extend along the entire anterior margin of the procoracoid cartilage (Stage 36, MACN 39896.ej3 and MACN 39896.ej4) and then overlaps the anterior half of the dorsal and ventral surfaces of the procoracoid (MACN 39896.ej4). By mid-metamorphosis (Stage 43), the lateral end of the clavicle completely overlaps the medial margin of the *pars acromialis* (Fig. 10D).

The coracoid cartilage has an incipient periosteal ossification at the middle of the diaphysis in some Stage-35 specimens (MACN 39895.ej4 and only on the right side in MACN 39895.ej3). The same occurs to the scapular cartilage, where the periosteal ossification is variable by Stage 35 (from two fifths in MACN 39895.ej1 and MACN 39895.ej3 to almost the complete diaphysis in MACN 39895.ej4). By Stage 38, the diaphyses of coracoid and scapula are well ossified. The scapular *partes glenoidalis* and *acromialis* remain cartilaginous until postmetamorphic stages. The ossified scapula of juveniles bears an incipient to well-formed anterior crest at the anterior margin of the diaphysis (Fig. 10E), which expands during postmetamorphic ontogeny.

The cleithrum reaches the leading edge of the suprascapular cartilage in Stage 35 and thereafter

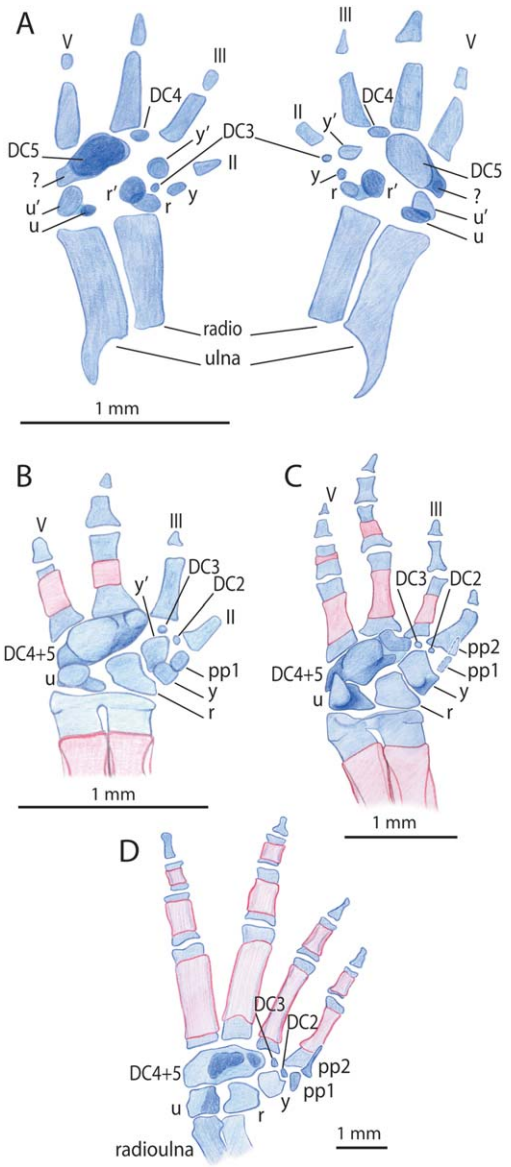

Fig. 11. *Calyptocephalella gayi*. Ontogeny of the manus. Left hand at Stage 34 in (**A**) palmar and (**B**) dorsal views (MACN 39894.ej1). Right hand in palmar view at (**C**) Stage 35 (MACN 39895.ej2), (**D**) Stage 37 (MACN 39897.ej1), and (**E**) Stage 39 (MACN 39899). Abbreviations: II–V = Digits II to V; DC = Distal Carpal; pp = prepollical element; r = radiale; r' = radiale'; u = ulnare; u' = ulnare'; y = Element Y; y' = Element Y'. Blue denotes cartilage, red denotes bone. Note the presence of a "?" element during the formation of DC 4 + 5, and the presence of two cartilaginous condensations for the formation of the radiale, ulnare, and Element Y.

increases rapidly in size. The dorsal surface of the cleithrum bears a keel along the lateromedial extent of the element, a feature that is evident from Stage 37 (Fig. 10C) onward.

Among the specimens examined, the omosternum and sternum are first observed in juveniles (Fig. 10E); the former element is small and fungiform, whereas the latter is relatively large, has nearly adult proportions, and is posteriorly bilobed.

Despite an incipient cartilaginous bridge that connects them distally, the radius and ulna remain discrete until Stage 37. The development of the compound radioulna occurs after the radius and ulna start to ossify independently in Stage 35; subsequently, their ossified diaphyses fuse with one another (incipient in MACN 39897.ej3), whereas their cartilaginous portions remain clearly separated. The radioulna is formed at Stage 39, and by Stage 40, the diaphyses of the humerus and radioulna are ossified, and only their epiphyses remain cartilaginous.

Remarkable changes occur in the carpal region between Stages 34 and 38, when the adult morphology is achieved (Fig.11). In Stage 35, the cartilaginous elements ulnare and ulnare', formerly separated and still identifiable, are embedded in a large, loose cartilaginous mass; the same is true for DCs 4 and 5. In contrast, radiale and radiale' are indistinguishably fused to form a single subrectangular element, the radiale. Two elements appear in Stage 35: DC 2, which consists of a small chondrification, and the basal element of the prepollex, located preaxial to Element Y and Element Y'. By Stage 36, chondrifications ulnare and ulnare' form a single element, the ulnare; the same occurs with Element Y and Element Y' that constitute Element Y, which is as large as the radiale. The loose cartilaginous mass that includes DCs 4 and 5 is more consolidated, uniting these chondrifications. Two additional prepollical elements appear aligned distal to the basal element of the prepollex—one at Stage 37 and another (an elongated chondrification) at Stage 38. Carpal torsion occurs in this stage; according to Jenkins and Shubin (1998), the carpal elements are twisted to realign proximal end of the radioulna. Ossification centers are present in the radiale, the ulnare, Element Y, and DC 4 + 5 in juveniles.

The four MtCs are present in Stage 35; MtCs IV and V start to ossify at this stage, whereas MtCs II and III begin periosteal ossification at Stage 37. The number of phalangeal elements varies among individuals (it may also vary between right and left manuses of the same specimen) until Stage 37, when the hand has the adult phalangeal formula (2 2 3 3). By Stage 36, Digit II starts to develop and Digit IV reaches its final shape. This sequence of development is repeated in the ossification of the phalangeal elements, starting at Stage 37 on Phalanx 1 of Digits III–V and on Phalanx 2 of Digit IV and ending at Stage 40, when all of the digital phalanges are ossified.

Pelvic girdle and hind limb. In Stage 34, the halves of the pelvic girdle are separated from one another by a distance equivalent to the width of the notochord; they lie ventral to the muscular tail of the tadpole and posterior to the distal end

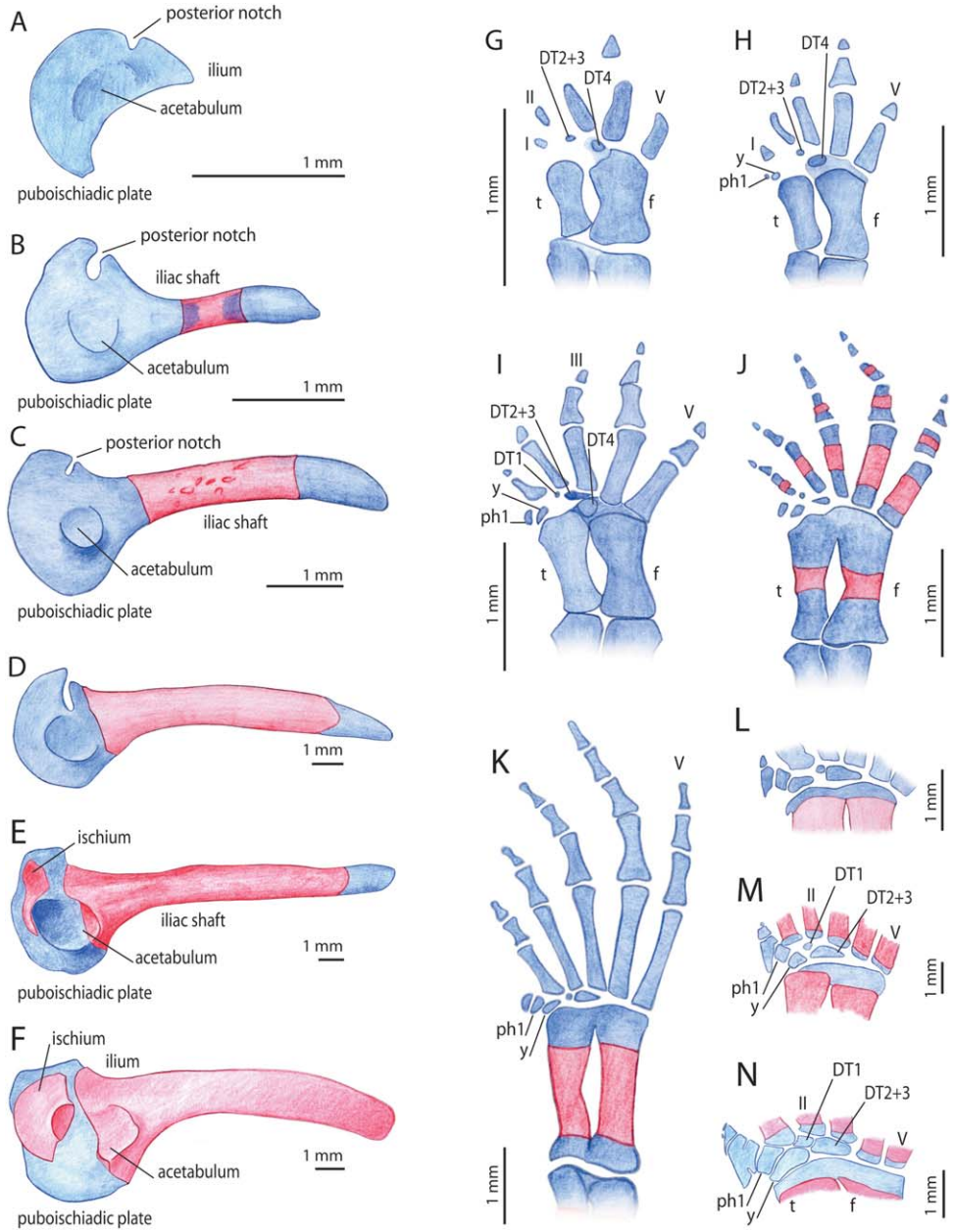

Fig. 12. *Calyptocephalella gayi*. Ontogeny of the pelvic girdle and tarsus. Pelvic girdle in lateral view at (**A**) Stage 34 (MACN 39894.ej1), (**B**) GS Stage (MACN 39895.ej2), (**C**) Stage 37 (MACN 39897.ej1), (**D**) Stage 39 (MACN 39899). (**E**) Stage 40 (MACN 39900), and (**F**) juvenile (MACN 48396). Right foot in dorsal view at (**G**) Stage 34 (MACN 39894.ej1), (**H**) Stage 35 (MACN 39895.ej2), (**I**) Stage 36 (MACN 39896.ej1), (**J**) Stage 37 (MACN 39897.ej1), (**K**) Stage 38 (MACN 39898.ej1), (**L**) Stage 39 (MACN 39899), (**M**) Stage 40 (MACN 39900), and (**N**) juvenile (MACN 48396). Abbreviations: I–V = Digits I to V; DT = Distal Tarsal; ph = prehallical element; f = fibulare; t = tibiale; y = Element Y. Blue denotes cartilage, red denotes bone. Note the development of the pelvic girdle from a single chondral element; the puboischiadic plate has a posterior notch at Stage 34, previous to the elongation of the ilium into an ilial shaft. The cartilaginous distal end of the fibulare bears the Distal Tarsal 4, discernible until Stage 36.

of the hypochord. Each half is semicircular in lateral aspect; the posterior margin is convex and the dorsal margin has a U-shaped notch ("posterior notch" of Green, 1931) (Fig. 12A). According to Green (1931), this notch marks the boundary between the dorsal and ventral elements—that is, the ilium and puboischiadic plate, respectively. In some specimens (MACN 39894.ej3 and MACN 39894.ej4), short ilial shafts are developed with traces of ossification in their central portions.The concavity of the acetabulum or *fossa acetabularum* for the articulation of the hind limb is scarcely discernible. The femoral cartilage has a curved concave margin and is slightly wider distally than proximally. The tibia and fibula cartilages are well-defined elements, the distal ends of which are

united by loose cartilage. The length of the latter elements is about two thirds that of the femoral cartilage. The femur, tibia, and fibula have traces of periosteal ossification at the central third of their diaphysis.The proximal tarsals—tibiale and fibulare—are well chondrified and half the length of the femoral cartilage. The tibiale is slightly shorter and distinctly thinner than the fibulare. The distal end of the fibulare has a mediodistal projection of loose cartilage, which includes an oval chondrification that develops therein (Fig. 12G–J). The latter chondrification extends to the bases of MtTs III and IV and is identified as the DT 4. Medial and distal to DT 4, DT 2 + 3 is present as a circular chondrification between the bases of MtTs II and III. MtTs II–V are present in all the specimens examined, whereas MtT I is barely chondrified. MtT IV is the best developed of the series. Two individuals (MACN 39894.ej1 and MACN 39894.ej2) have the first phalanx of Digit IV, and MACN 39894.ej2 also has the first phalanx of Digit V. None of the autopodial elements have traces of ossification.

Throughout development, the pelvic girdle rotates gradually, changing its position relative to the axial column. In lateral view, the ilial shaft shifts its orientation, from dorsal (at Stage 34) to dorsoanterior (at Stage 39); ultimately, the entire pelvic girdle comes to be situated ventral to the notochord and posterior to the NAs X and XI. By Stage 40, the ilial shafts parallel the axial column, and by Stage 43, they reach the sacral diapophyses. The articulation between the pelvis and the axial column is well established in postmetamorphic individuals, when the sacral diapophyses are well developed. In dorsal aspect, it is evident that the plates (i.e., the posterior round portions) of the pelvic girdle progressively approximate one another. Thus, by Stage 36, the right and left ischiadic portions remain separated but are four times closer to each other than are the ilial portions. At Stage 39, the controlateral puboischiadic plates are in contact distally, thereby imparting a V shape to the pelvic girdle; by Stage 43, these plates as well as the acetabular portions of the ilia are in medial contact.

The ilium has developed an ilial shaft in all specimens examined at Stage 35; it is half the length of the body of the pelvic girdle. By Stage 37, the shaft has increased in length to two and a one-half times the length of the body of the pelvic girdle, a ratio that persists in the adult (Fig. 12C–F). Ilial ossification begins in the mid–third of the shaft at Stage 35; the bone achieves 60% of its length by Stage 37 and forms the base of the iliac body by Stage 38. By Stage 40, ossification extends to the anterior margin of the posterior notch, the anterior margin of the acetabulum and part of the acetabular fossa. At this stage, the ilial shaft has a low crest along the posterior two thirds of its dorsal margin (Fig. 12E); subsequently, the ilial crest increases in length in proportion to the ilial shaft. In contrast, the size of the dorsal crest increases rapidly to one third of the height of the ilial shaft in juvenile stages. In postmetamorphic individuals, the ilial ossification extends posteriorly to form one third of the acetabular fossa. The ischium is first observed at Stage 40 (Fig. 12E), posterodorsal to the acetabular fossa. In postmetamorphic individuals, it is well ossified, forming more than one third of the puboischiadic plate, including part of the acetabular fossa and the posterodorsal margin (Fig. 12F). No ossification that might correspond to the pubis was observed in any of the developmental stages.

The femoral cartilage has a periosteal ossification along the complete diaphysis at Stage 37, whereas the spherical proximal head and the distal end are cartilaginous; the proximal head continues to develop in association with the acetabular fossa. At Stage 39, an incipient ventral crest is visible on the ventral surface of the femoral diaphysis. The tibia and fibula cartilages are united at their proximal ends by means of a cartilaginous bridge in Stage 37; the fusion of their ossified diaphyses is delayed until the last stages of metamorphosis. The diaphyses of all of the hind-limb bones are ossified by Stage 40, but their epiphyses remain cartilaginous. In postmetamorphic individuals, the hind limb is twice the length of the forelimb.

The proximal tarsals are united distally by a cartilage that extends along the distal margin of the fibulare to the laterodistal corner of the tibiale in Stage 36 (Fig. 12I), when the tibiale is half as wide as the fibulare and expanded at both proximal and distal ends. The distal end of the fibulare is more chondrified than in previous stages and, by Stage 37, DT 4 is no longer visible as a distinct chondrification (Fig. 12J). Element Y and the proximal element of the prehallux are first observed at Stage 35; the former is an incipient, spherical chondrification next to the anteromedial margin of the tibia, whereas the prehallical element is medial and distal to the Element Y. The first phalanx of Digits III–V and the second phalanx of Digits III and IV also are present. DT 1 is added to the autopodium in Stage 36; it consists of a spherical chondrification between the bases of MtTs I and II. The shape of DT 2 + 3 has changed from spherical to triangular, with the element being wedge under MtT II; a spherical, darker-staining element observed within the taller side of this triangular chondrification may correspond to DT 2. The prehallux is composed by three elements, which are formed between Stages 38–40 (Fig. 12K–M); the second prehallical element (ph2) becomes spur-shaped, with the acuminate end reaching the level of the proximal tarsals (Fig.

12N); this morphology prevails in adults (see Fig. 6E).

The ossification is periosteal in all of the autopodial elements, except the distal tarsals. The proximal tarsals, MtTs III–V and first phalanges of Digits IV and V start to ossify on the central portion of their respective diaphyses in Stage 36. Later, by Stage 37, the central portion of each of the five metatarsals is already ossified. The central portion of phalanges ossify in Stage 38, except for the distal ones, which ossify at Stage 39. In postmetamorphic individuals, the epiphyses of all of the hind-limb elements, as well as the distal tarsals, Element Y, and the prehallux remain cartilaginous.

DISCUSSIONS

The few available anatomical studies hint at the considerable diversity in Myobatrachoidea and the uncertainties that remain with respect to their evolutionary history. This lack of morphological and developmental data makes it difficult to establish meaningful comparisons with their South American relatives. The osteological observations made on specimens housed at KU (indicated as pers. obs.) are included herein to supplement the scarse information in the literature.

Comparative Morphology of the Adult Postcranial Skeleton

In *C. gayi*, the atlas and second presacral vertebra are discrete, in contrast to *Telmatobufo*, in which the two vertebrae are fused (Lynch, 1978; Formas et al., 2001; pers. obs.). The fusion of PVs I and II is a character that has been evaluated in the few analyses of the relationships within Myobatrachoidea based on morphology (Heyer and Liem, 1976). Davies (2003) agreed with Littlejohn et al. (1993) in the fact that the fusion of the first two vertebrae supports Limnodynastidae, although *Mixophyes*, included in this group at that time, was mentioned as an exception. However, under current phylogenetic hypotheses (in which *Mixophyes* and *Rheobatrachus* constitute Myobatrachidae taxa—Frost et al., 2006; Pyron and Wiens, 2011), the clade Limnodynastidae has these vertebrae fused, whereas the opposite condition occurs in Myobatrachidae (Table 3). Fusion of the atlas and PV II occurs occasionally among anomocoelans and at the base of Neobatrachia (e.g. *Hadromophryne natalensis*, Lynch, 1971; pers. obs.), but the general condition within Ranoidea and Hyloidea is the presence of discrete elements. It is noteworthy that a change of condition seems to have occurred at least twice within Australobatrachia (once in Calyptocephalellidae and once in Myobatrachoidea, Fig. 13).

The great expansion of the sternal elements (i.e., omosternum and sternum) is a distinctive feature of the pectoral girdle of *C. gayi*. The omosternum of *Telmatobufo* is also a well-developed, anteriorly expanded element, according to Schmidt (1952) and Formas et al. (2001). However, Parker (1940) and Lynch (1971) reported that among Limnodynastidae and Myobatrachidae, the occurrence of an omosternum was variable. Additionally, Lynch (1971) observed that, when the omosternum is present, it is small, except in *Mixophyes*; this concurs with observations by Keferstein (1868) who reported the presence of a weak omosternum in *Limnodynastes dumerili*, *Crinia signifera* (as *C. georgiana*)[1], *C. tasmaniensis*, *Geocrinia* (as *Crinia*) *laevis*, and *Platyplectrum ornatum* (as *P. marmoratum*). However, Anderson (1916) described the omosternum of *Lechriodus* (as *Phanerotis*) *fletcheri* as a well-developed, cartilaginous, long narrow style, while the illustrations of Keferstein (1868) show the omosterna of *Mixophyes fasciolatus* and *Heleioporus albopunctatus* (*H. australiacus*, according to Moore, 1961) as a long, spatulate structure. The omosternum was also described as elongated in *Assa darlingtoni* (Tyler, 1972), long and slender in *Mixophyes hihihorlo* (Donnellan et al., 1990), but slim and short in *Rheobatrachus* (Davies and Burton, 1982; Mahony et al., 1984). We confirm the presence of omosternum in *Notaden nichollsi*, *Platyplectrum ornatum*, *Adelotus brevis*, *Crinia signifera*, *C. bilingua*, *Uperoleia fusca*, and *Pseudophryne bibroni* (pers. obs., Fig. 14); in these species, except in the latter taxon, the omosternum is a relatively elongated and large structure. Additionally, in *Adelotus brevis* it is anteriorly expanded (Keferstein, 1868; pers. obs.). The omosternum was reported as absent in the fossorial species *Myobatrachus gouldi* and *Arenophryne rotunda*, as well as *Pseudophryne guentheri* (Tyler, 1976b; Davies, 1984). The presence of an omosternum seems to be variable in *Pseudophryne*, according to the aforementioned data and observations. The omosternum is either present or absent in *Uperoleia* also; it is present in *U. russelli* (Stephenson, 1965), *U. aspera* and *U. mjorbergi* (Tyler et al., 1981), *U. grandulosa* and *U. altissima* (Davies and Roberts, 1985; Davies et al., 1993), but it is absent in *U. rugosa* (Davies and Mc Donald, 1985), *U. laevigata*, *U. martini*, and *U. tyleri* (Davies and Littlejohn, 1986).

The sternum is conspicuous in *C. gayi*, being as long as the omosternum plus the epicoracoid. Despite its large size, it is cartilaginous in all but the largest individuals examined in which some loose mineralizations are present. The sternum of *Telmatobufo* is also large, but, in contrast to that of *C. gayi*, it is extensively mineralized in the

[1]According to Parker (1940), it corresponded to an individual of *Taudactylus acutirostris*. Unfortunately, it was not possible to asses the presence or absence of the omosternum in *T. acutirostris* from KU 124233.

TABLE 3. Condition of fused or unfused presacral vertebrae I and II within Australobatrachia

Species	PV I, PV II	Source
Adelotus brevis	Not fused	Lynch, 1971; pers.obs.
Arenophryne rotunda	Fused	Davies, 1984
Assa darlingtoni	Fused	Tyler, 1972
Calyptocephalella gayi	Not fused	Lynch, 1971; pers.obs.
Crinia bilingua	Fused	pers.obs
Crinia signifera	Fused	Lynch, 1971
Heleioporus australiacus	Not fused	Lynch, 1971
Heleioporus eyrei	Not fused	Lynch, 1971
Lechriodus aganoposis	Not fused	Zweifel, 1972
Lechriodus fletcheri	Not fused	Zweifel, 1972
Lechriodus melanopyga	Not fused	Zweifel, 1972
Lechriodus platyceps	Not fused	Zweifel, 1972
Lechriodus spp.	Fused	Lynch, 1971; Parker, 1940
Limnodynastes dorsalis	Not fused	Lynch, 1971
Limnodynastes fletcheri	Not fused	Lynch, 1971
Limnodynastes peroni	Not fused	Lynch, 1971; pers.obs.
Limnodynastes tasmanensis	Not fused	Lynch, 1971
Metacrinia nichollsi	Fused	Lynch, 1971
Mixophyes fasciolatus	Fused	Lynch, 1971; pers.obs
Mixophyes hihihorlo	Fused	Donnellan et al., 1990
Mixophyes schevilli	Fused	Wu, 1994
Myobatrachus gouldii	Fused	Lynch, 1971; Davies, 1984; pers.obs
Neobatrachus aquilonius	Not fused	Lynch, 1971 (as *N. centralis*); pers.obs.
Neobatrachus pictus	Not fused	Lynch, 1971; pers.obs.
Notaden bennetti	Not fused	Lynch, 1971
Notaden nichollsi	Not fused	Lynch, 1971; Wu, 1994; pers. obs.
Philoria frosti	Not fused	Lynch, 1971; pers.obs.
Philoria sphagnicolus	Not fused	Lynch, 1971 (as *Kyarranus*)
Platyplectrum ornatum	Not fused	pers.obs
Pseudophryne bibroni	Fused	Lynch, 1971; pers.obs.
Pseudophryne corroboree	Fused	Lynch, 1971
Pseudophryne douglasi	Fused	Davies, 1984
Pseudophryne occidentalis	Fused	Tyler and Davies, 1980
Rheobatrachus silus	Fused	Davies and Burton, 1982
Rheobatrachus vitelinus	Fused	Mahony et al., 1984
Taudactylus acutirostris	Fused	Lynch, 1971; pers.obs.
Taudactylus diurnus	Fused	Wu, 1994
Telmatobufo	Fused	Lynch, 1978; Formas et al., 2001
Uperoleia altissima	Fused	Davies et al., 1993
Uperoleia fusca	Fused	pers.obs.
Uperoleia grandulosa	Fused	Davies and Roberts, 1985
Uperoleia laevigata	Fused	Davies and Littlejohn, 1986
Uperoleia martini	Fused	Davies and Littlejohn, 1986
Uperoleia mjorbergi	Fused	Tyler et al., 1987
Uperoleia rugosa	Fused	Lynch, 1971; Davies and Littlejohn, 1986; pers.obs.
Uperoleia ruselli	Fused	Lynch, 1971 (as *Glauertia*); pers.obs.
Uperoleia tyleri	Fused	Davies and Littlejohn, 1986

three species for which the osteological description is available (Schmidt, 1952; Lynch, 1971; Formas et al., 2001; pers. obs.). The notch on the posterior margin of the sternum of *C. gayi* also occurs in *Telmatobufo*, although it is shallower in the latter taxon. The notch is also present in *Platyplectrum ornatum* (pers. obs.; Fig. 14C), *Mixophyes fasciolatus, Heleioporus australiacus* (Keferstein, 1868, Taf. V, Figs. 4 and 6), and the basal neobatrachian *Hadromophryne natalensis* (pers. obs.; Fig. 14A). The sternum is also proportionally large and wide in several myobatrachids, such as *Rheobatrachus silus* (Davies and Burton, 1982), *R. vitelinus* (Mahony et al., 1984), *Pseudophryne guentheri* (Tyler, 1976b), *P. douglasi, P. coriacea, P. semimarmorata*, (Davies, 1984; Littlejohn et al., 1993), *P. bibroni* (pers. obs.), *Arenophryne rotunda* (Tyler, 1976b), *Notaden nichollsi*, *Crinia signifera*, *C. bilingua, Adelotus brevis*, *Uperoleia fusca* (pers. obs.), *U. ruselli* (Stephenson, 1965), *Mixophyes fasciolatus* (Keferstein, 1868), *M. hihihorlo* (Donnellan et al., 1990), and *Heleioporus australiacus* (Keferstein, 1868). In contrast, the sternum of *Myobatrachus gouldii* is slim and relatively small (Littlejohn et al., 1993, pers. obs.), as well as that of *Assa darlingtoni*, which is small although slightly expanded anteriorly. The sternum is entirely cartilaginous in all myobatrachoids (Lynch, 1971), although

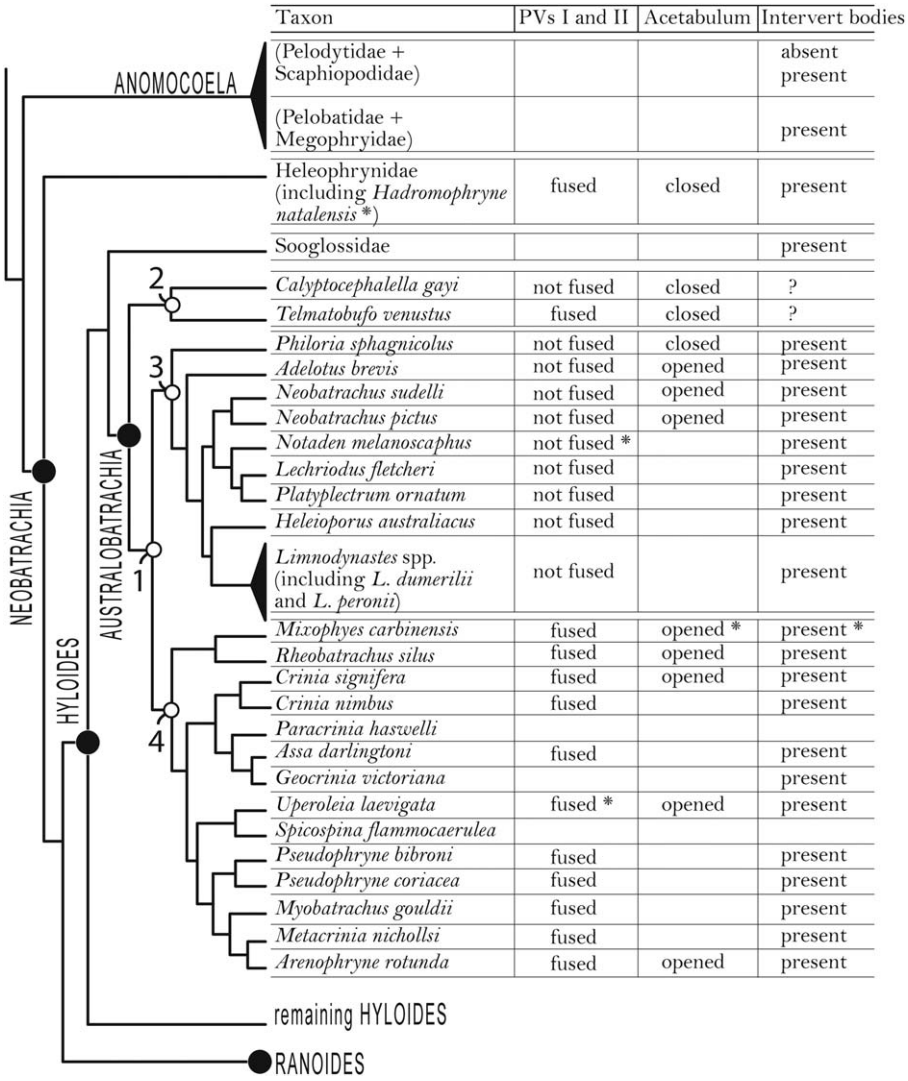

Taxon	PVs I and II	Acetabulum	Intervert bodies
(Pelodytidae + Scaphiopodidae)			absent present
(Pelobatidae + Megophryidae)			present
Heleophrynidae (including *Hadromophryne natalensis* *)	fused	closed	present
Sooglossidae			present
Calyptocephalella gayi	not fused	closed	?
Telmatobufo venustus	fused	closed	?
Philoria sphagnicolus	not fused	closed	present
Adelotus brevis	not fused	opened	present
Neobatrachus sudelli	not fused	opened	present
Neobatrachus pictus	not fused	opened	present
Notaden melanoscaphus	not fused *		present
Lechriodus fletcheri	not fused		present
Platyplectrum ornatum	not fused		present
Heleioporus australiacus	not fused		present
Limnodynastes spp. (including *L. dumerilii* and *L. peronii*)	not fused		present
Mixophyes carbinensis	fused	opened *	present *
Rheobatrachus silus	fused	opened	present
Crinia signifera	fused	opened	present
Crinia nimbus	fused		present
Paracrinia haswelli			
Assa darlingtoni	fused		present
Geocrinia victoriana			present
Uperoleia laevigata	fused *	opened	present
Spicospina flammocaerulea			
Pseudophryne bibroni	fused		present
Pseudophryne coriacea	fused		present
Myobatrachus gouldii	fused		present
Metacrinia nichollsi	fused		present
Arenophryne rotunda	fused	opened	present

Fig. 13. Distribution of morphological traits mapped onto a phylogenetic hypothesis of Australobatrachia simplified from Frost et al. (2006). Node 1: Myobatrachoidea; Node 2: Calyptocephalellidae; Node 3: Limnodynastidae; Node 4: Myobatrachidae. The asterisk (*) indicates data coded from a different, although closely related, species.

occasionally in a few taxa some individuals have been reported as having some mineralizations (Parker, 1940; *Rheobatrachus vitelinus*, Mahony et al., 1984; *Mixophyes hihihorlo*, Donnellan et al., 1990; *Myobatrachus gouldii*, pers. obs.). The significant variation in the sternal structures within Australobatrachia may be related to the widely divergent habits of the members of this group, which include aquatic, fossorial and arid-inhabitant species (Littlejohn et al., 1993; Anstis, 2013).

The presence of a prominent crest along the anterior margin of the scapula is another distinct feature of the pectoral girdle of *C. gayi*. The crest develops postmetamorphically and is conspicuous in adults. The name of the structure was initially given to the lamina along the leading edge of the scapula of *Pelobates cultripes* and *Lithobates catesbeianus* (as *Rana catesbyana*; Bolkay, 1919), but this feature is present in many taxa across the anuran tree, such as the costatan *Bombina maxima and Discoglossus sardus* (Púgener and Maglia, 1997), the anomocoelan *Pelodytes punctatus* (Procter, 1921) and *P. ibericus* (Sanchiz et al., 2002), and the neobatrachian *Hadromophryne natalensis* (pers. obs., Fig. 15A), *Pseudis paradoxa* (Procter, 1921), *Telmatobius rubigo* (Barrionuevo and Baldo, 2009), and *T. oxycephalus* (Barrionuevo, 2013). Among australobatrachians, it was observed in *Telmatobufo venustus* (pers. obs., Fig. 15E), *Rheobatrachus silus* (Davies and Burton, 1982), *R. vitelinus* (Mahony et al., 1984), *Pseudophryne bibroni*, *Myobatrachus gouldii*, *Crinia signifera*, *C. bilingua*, and *Limnodynastes tasmaniensis* (pers. obs., Fig. 15B,F). In contrast, the scapula lacks an anterior crest in *Taudactylus acutirostris*, *Uperoleia fusca, U. ruselli*, *U. rugosa,*

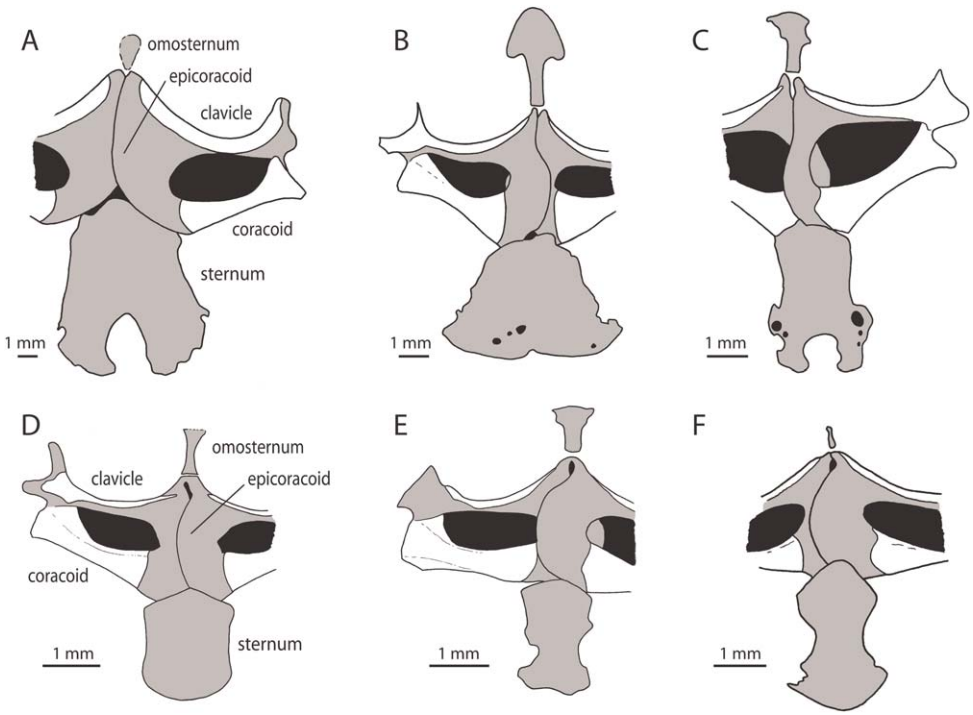

Fig. 14. Pectoral girdle, ventral view. (**A**) *Hadromophryne natalensis* (KU 195926), (**B**) *Adelotus brevis* (KU 179912), (**C**) *Platyplectrum ornatum* (KU 179936), (**D**) *Crinia signifera* (KU 56348), (**E**) *Uperoleia fusca* (KU 180028), and (**F**) *Pseudophryne bibroni* (KU 93588). Gray denotes cartilage, white denotes bone, black indicates the fenestra.

Neobatrachus pictus, *N. aquilonius*, *Notaden nichollsi*, *Platyplectrum ornatum*, *Adelotus brevis*, *Philoria frosti*, and *Limnodynastes dumerilii* (pers. obs., Fig. 15C,D,G). The extent of the anterior crest, however, varies among the taxa in which it is present. In most australobatrachians, the anterior crest is short and restricted to the *pars acromialis*. In *C. gayi* and *Pseudophryne bibronii*, the crest extends along the shaft between the anteromedial (anteroventral) and the anterolateral (anterodorsal) ends of the scapula, as it does in *Pelodytes punctatus, P. ibericus, Pseudis paradoxa*, *Telmatobius rubigo*, and *T. oxycephalus* (op.cit.).

Adult australobatrachians have two basic morphological types of pelvic girdle; in one case, the bottom of the acetabular fossa is completely closed by cartilage, whereas in the other, the acetabular fossa has an irregular opening at its center. *Telmatobufo* and *C. gayi* have closed acetabular fossae, as apparently do *Philoria* (as *Kyarranus*) *sphagnicolus*, for which Tyler (1976a:9) reported "... only the central portion of the acetabular fossa remaining cartilaginous." In contrast, an open acetabular fossa was observed in species of *Neobatrachus*, *Adelotus brevis*, *Philoria frosti*, *Taudactylus acutirostris* (pers. obs.), *Uperoleia* species (Davies and Littlejohn, 1986; Davies et al., 1993; pers. obs.), *Rheobatrachus silus* (Davies and Burton, 1982), *R. vitelinus* (Mahony et al., 1984), *Arenophryne rotunda* (Davies, 1984), and *Mixophyes hihihorlo* (Donnellan et al., 1990).

Developmental Aspects

Several developmental features of the postcranial skeleton of *C. gayi* are of interest, either because of their unusual occurrence among anurans or because of their significance as a baseline to the study of other australobatrachian taxa in the search for osteological synapomorphies that support the clade.

The study of the osteogenesis of the axial skeleton has revealed peculiar aspects in the development of vertebral centra. The contribution of an additional ventromedial ossification during the formation of the perichordal ring at the centrum of PV VIII (see figures in Additional Supporting Information) is a condition that, to our knowledge, has not been reported previously. However, a ventromedial center of ossification is involved in the ossification of all the presacral vertebral centra (i.e., not only PV VIII) of phylogenetically distant neobatrachians, the hylids *Litoria rheocola* and *L. nannotis*, and the arthroleptid *Leptopelis vermiculatus* (Haas, 2003). In turn, two dorsolateral and two ventrolateral (with respect to the notochord) ossification centers were described for the ossification of supernumerary postsacral vertebrae in the larvae of some megophryid anomocoelan species (*Megophrys stejnegeri*, *M. lateralis*, *Ophryophryne microstoma*, *Leptolalax pelodytoides*, and *Xenophrys* sp.), a pattern that was named "Bogenbasen mode" (Handrigan et al., 2007). Also, two pairs of ossification centers were described in

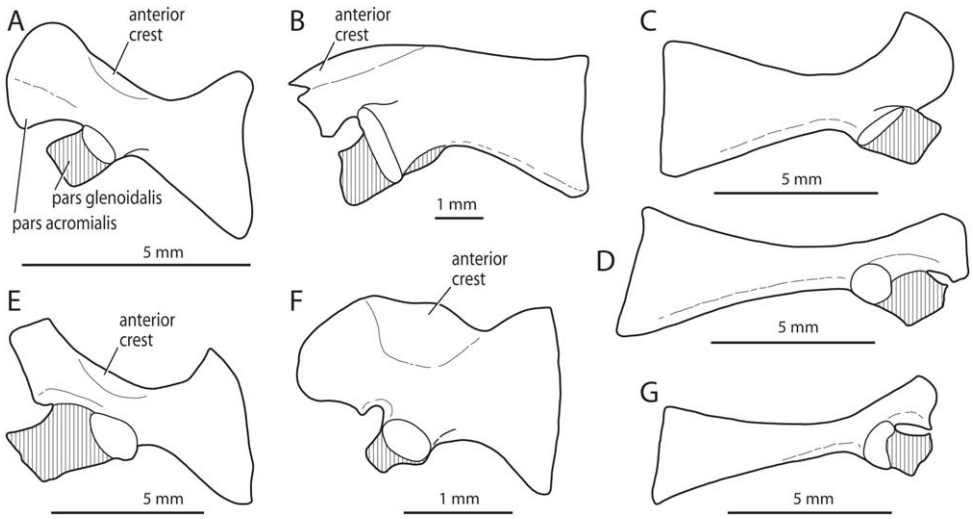

Fig. 15. Scapula, ventral view. (**A**) *Hadromophryne natalensis* (KU 195926), (**B**) *Myobatrachus gouldii* (KU 110333), (**C**) *Notaden nichollsi* (KU 93581), (**D**) *Neobatrachus aquilonius* (KU 93578), (**E**) *Telmatobufo venustus* (KU 161439), (**F**) *Pseudophryne bibroni* (KU 93588), and (**G**) *Neobatrachus pictus* (KU 69278). Hatching of the *pars glenoidalis* indicates the deeper region of the glenoid cavity. Note the presence/absence of an anterior crest in the different taxa.

the formation of the presacral centra of *Batrachyla taeniata*, a hyloid neobatrachian (Alcalde, 2007). The lack of developmental studies of the postcranial skeleton of australobatrachians limits our ability to describe a pattern of ossification of the vertebral centra in this group. However, morphological features of the centrum of PV VIII (and no other) of a young adult of *Limnodynastes peronii* (KU 93566) might be interpreted as resulting from the fusion of a dorsal perichordal arch to a single, ventral ossification (pers. obs., Fig. 16A). If correct, this species and *C. gayi* would be the only two taxa for which three ossification centers are reported to take place during the formation of the bony centrum of PV VIII. It should be noted that the midventral transient constrictions observed in PVs I–VII in the ontogeny of *C. gayi* are interpreted as evidence that each perichordal ring is formed only by two dorsolateral ossification centers. The latter has been reported as the general developmental pattern of the axial skeleton for neobatrachians (e.g., *Amietophrynus regularis*, Sedra and Moursi, 1958; *Ceratophrys cornuta*, Wild, 1997; *Chacophrys pierotti*, Wild, 1999; *Acris crepitans*, Pugener and Maglia, 2009) as well as for anomocoelans (*Pelobates cultripes* and *Pelodytes punctatus*, Talavera, 1990; *Spea*—as *Scaphiopus—intermontana*, Hall and Larsen, 1998; *S. multiplicata*, Banbury and Maglia, 2006).

Historically, the presence of free intervertebral discs between successive presacral centra in subadults has been one of the features highlighted as prevalent among Australopapuan "leptodactylids." This condition was used by several authors (e.g., Lynch, 1973; Littlejohn et al., 1993) to characterize the Myobatrachidae (sensu Duellman and Trueb, 1994), but examination of the literature reveals contradictory information on its distribution. Parker (1940:8) pointed out that *Heleioporus*, *Mixophyes*, *Limnodynastes*, *Notaden*, *Adelotus*, *Uperoleia* (as *Glauertia and Uperoleia*), *Crinia*, *Myobatrachus*, *Pseudophryne*, and *Metacrinia* have "an incomplete fusion of the intervertebral condyle with the vertebra." Subsequently, this condition was noted in *Neobatrachus* (Lynch, 1971), *Assa*, *Geocrinia*, and *Taudactylus* (Heyer and Liem, 1976). However, Heyer and Liem (op. cit.) scored *Heleioporus*, *Mixophyes, Limnodynastes*, *Neobatrachus*, and *Notaden*, along with *Philoria*, *Platyplectrum*, *Rheobatrachus*, and *Lechriodus* as having procoelous vertebrae resulting from the ankylosis of each intervertebral disc to the anterior adjacent vertebral centrum. Parker (1940) and Heyer and Liem (1976) agreed that the vertebral bodies of the latter genus lack notochordal pits, whereas the condyles are firmly ankylosed to the centra. Davies (1984) mentioned that free intervertebral discs occur in *Arenophryne rotunda* during its ontogeny, and Littlejohn et al. (1993:12) reported that "...the majority of [Limnodynastinae] genera have free intervertebral discs as subadults" and that "...[in Myobatrachinae] the vertebrae are procoelous with free intervertebral discs in many cases persisting in the adult." Also Talavera (1990) indicated that species of Myobatrachidae together with those of Pelobatidae and Megophryidae are the only anurans having free condyles in at least some period of their life cycles.

From the foregoing and the observations made on specimens housed at KU, it follows that the

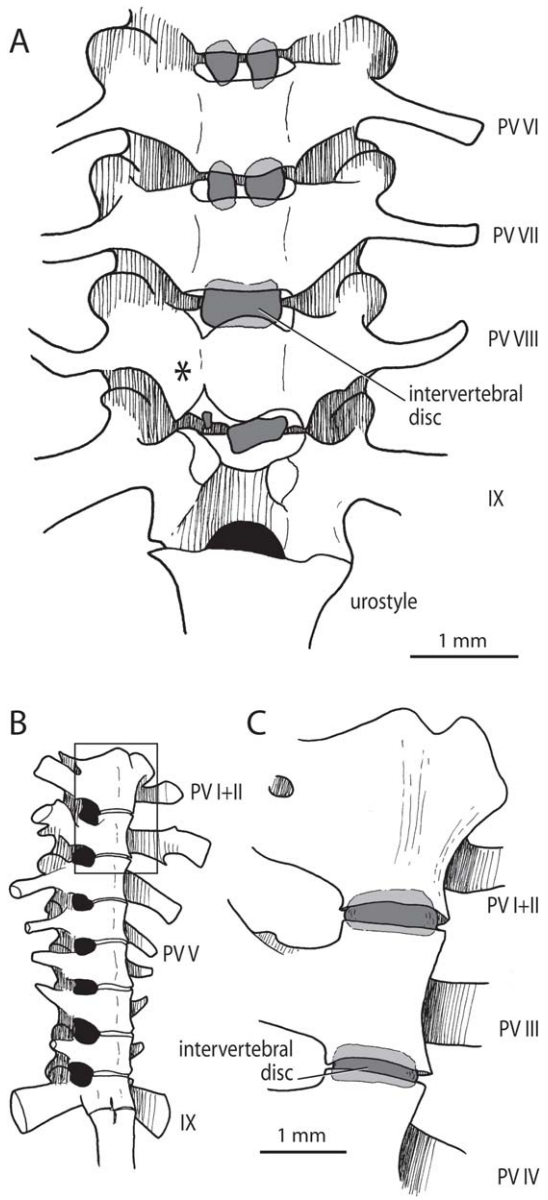

Fig. 16. Axial skeleton. (**A**) *Limnodynastes peroni* (KU 93566) and (**B**, **C**) *Neobatrachus pictus* (KU 69278). Abbreviation: PV = Presacral Vertebra. Note the constriction (*) on the centrum of Presacral Vertebra VIII, which indicates the place where the ventromedial and dorsal ossification centers fuse to form the perichordal ring. The presence of intervertebral discs is evident in both taxa.

contradictory data in the literature probably resuts from the different developmental stages of the individuals examined. However, it is the presence of these free intervertebral discs during some stage of the development and not the free condition of these discs in the adult that constitutes evidence of a distinctive developmental pattern. The intervertebral discs in australobatrachids look like small osseous balls between consecutive vertebral centra (pers. obs., Fig. 16B). They are especially evident in *Neobatrachus pictus* (KU 69278), *Philoria frosti* (KU 50699), *Limnodynastes peroni* (KU 93566), and *Uperoleia rugosa* (KU 109861), in which the intervertebral discs are free (Fig. 15). They are also evident in *Adelotus brevis* (KU 147213, KU 186773) and in *Mixophyes fasciolatus* (KU 56627, KU 147227), in which, additionally, the discs are attached to the posterior ends of the vertebral centra.

There is not much information about the emergence of the ball and socket articulation between consecutive centra. In their classical histological work, Mookerjee and Das (1939) described that the chondrified perichordal tube of the intervertebral portion is split into a condyle and socket by a strand of migratory connective tissue cells. Sedra and Moursi (1958), however, did not confirm this mechanism; instead, they described that the joint arises by direct division of the tissue into two parts without the migration of any connective tissue strand. Nonetheless, neither of these patterns seems to be present in the hylid *Acris crepitans*, in which Pugener and Maglia (2009) did not find evidence of intervertebral cartilages and the developing centra are procoelous when they first form. These authors suggested that either the intervertebral cartilage fuses to the centrum early in development or the intervertebral cartilage is absent and the articular condyle is generated from the centrum. This pattern recalls that of *Pelodytes punctatus* as described by Talavera (1990), in which from Stage 43 onward, the vertebral centra are ossified and slightly concave at their anterior ends and slightly convex at their posterior ends (no ossification centers observed at the condyle); by the end of the metamorphosis the specimens have clear procoelous vertebrae. Apparently, the same pattern takes place in the pipid *Xenopus muelleri*; at Nieuwkoop and Faber Stage 58, the centra (particularly PVs III-V) have slightly convex anterior margins, whereas the posterior margins are concave (Pugener, 2002).

Unfortunately, we were unable to assess if free intervertebral discs occur in the development of the axial skeleton of *C. gayi* owing to the lack of appropriate developmental stages, and there is no information on the condition in *Telmatobufo*. Furthermore, the hyperossification of these two taxa results in adult centra for which it is impossible to infer whether intervertebral discs have been present. Despite this drawback, the presence of dry, ring-shaped, isolated cartilages between the vertebral centra in a dry skeleton of a young juvenile of *C. gayi* (MACN 45751) suggests that the presence of free intervertebral discs is plausible.

Free intervertebral discs have been described during the development in many anomocoelans. In the megophryids *Leptolalax pelodytoides* at Stage 45 and *L.* (as *Megophrys) lateralis* at Stage 46 these elements are present in cartilage (Handrigan and Wassersug, 2007). In the scaphiopodid

Spea intermontana (as *Scaphiopus intermontanus*), ossification of the free cartilaginous intervertebral discs begins at Stage 46 from as many as four different centers that eventually fuse to form the complete subespherical bony intervertebral disc (Hall and Larsen, 1998). In *S. bombifrons*, the spherical intervertebral discs chondrify and are visible between biconcave centra after metamorphosis, but their ossification occurs in young adults and remnants of the notochord persist in their centers (Wiens, 1989). In the aforementioned species of *Spea*, discs do not fuse to the centra, although they may adhere to either of the adjacent centra (Wiens, 1989; Hall and Larsen, 1998). According to Talavera (1990), young adult *Scaphiopus couchii* have free intervertebral discs. The pelobatid *Pelobates cultripes* has intervertebral discs that ossify from two ossification centers. The ossified discs remain free in subadults, but they fuse to the posterior end of the adjacent vertebra in the year following metamorphosis; no sutures remain in the adult (Talavera, 1990). Again, the lack of developmental data for Myobatrachoidea precludes us from knowing the pattern of ossification of the intervertebral discs in this group. Yet, in some of the specimens examined (*Philoria frosti* KU 50699, *Uperoleia rugosa* KU 109861, and *Limnodynastes peroni* KU 93566; Fig. 15A), the intervertebral discs appear to consist of two mineralized elements; whether this was an artifact of the stained specimens or the standard condition of the discs can not be determined but demands additional (e.g., histological) analyses.

The basal neobatrachian *Heleophryne* was considered as having amphicoelous vertebral centra (Heyer and Liem, 1976) whereas Lynch (1971:103–104) described "...a paedomorphic condition in which the tissue of the intervertebral body is not divided by invading arc of connective tissue"; he cited Griffiths (1959) as indicating that a similar condition occurs in the sooglosids *Nesomantis* and *Sooglosus*. However, the examination of an adult specimen of *Hadromophryne natalensis* (KU 195926) has revealed the presence of ossified intervertebral discs (pers. obs.).

Within Neobatrachia, the bufonid *Pedostibes hosii* was described as having procoelous centra formed by the fusion of the ossified intervertebral discs to the posterior ends of the centra (Pugener, 2002). In contrast, Sedra and Moursi (1958) described the presence of intervertebral cartilages in *Amietophrynus* (as *Bufo*) *regularis* that split into condyle and cotyle and fuse to the successive centra before any ossification in the intervertebral region occurs. Unfortunately, not much information is available for the neobatrachian clade, but when plotting the character on the anuran tree, we see that the free intervertebral discs might be a plesiomorphic condition for Neobatrachia. Additional observations of this trait in different developmental stages in neobatrachians appear crucial.

In anurans, the fusion of the independent chondrifications of coracoid, procoracoid, and scapular-suprascapular complex (the latter formed by two chondrifications) during early developmental stages results in the formation of each half of the pectoral girdle as a continuous cartilaginous structure, according to Baleeva (2001) and Havelková and Roček (2006). The epicoracoid cartilage develops from the chondrification of a mesenchymatous mass that links the procoracoid and the coracoid cartilages. The epicoracoid could grow either from any of the latter two or from both of them, depending on which of the cartilages develop first and on a differential distribution of the aforementioned mesenchymatous mass (Baleeva, 2009). In the earliest stage of *C. gayi* examined (Stage 34) there is a continuous cartilaginous structure in which coracoid, procoracoid, scapular, and suprascapular cartilages can be identified; the number of chondrification centers that gave rise to the girdle could not be determined. However, it was possible to observe the subsequent formation of the epicoracoid cartilage, which seems to develop from the procoracoid cartilage.

The adult carpus of *C. gayi*, composed of seven elements, originates from at least 12 cartilaginous anlage: two anlage each for the radiale, the ulnare, and the Element Y, three anlage to form the DC 4 + 5, and one for each of DC 3, DC 2, and the proximal element of the prepollex (pp1). At Stage 38, the adult formula is established and corresponds to the Type B of the 10 adult carpal morphologies described by Fabrezi (1992). *C. gayi* shares this carpal type with the australobatrachian *Telmatobufo venustus*, *Crinia signifera*, and *Taudactylus diurnus*, along with the pelodytid *Pelodytes punctatus*, among the large set of neobatrachian and non-neobatrachian taxa examined by Fabrezi (1992). She also reported this morphology in other neobatrachian taxa, such as Arthroleptidae (Hyperoliinae and Astylosterninae) and Sooglossidae (cited in Fabrezi, 1992). Fabrezi (op. cit.) provided a detailed description of the development of the carpal elements on several anuran species, among which she included *Telmatobufo venustus*, making the comparison with *C. gayi* possible. The origin of the carpal elements is the same in the latter two species. The most important shared character is the presence of a third cartilaginous nucleus (labeled with a "?" by Fabrezi) that is lateral to the large DC 5 and involved in the formation of the DC 4 + 5; this feature has been described only in *T. venustus* and *C. gayi*. In the other species examined, a compound DC 4 + 5 originates by the fusion of only two chondral elements, DC 4 and DC 5 (Fabrezi, 1992; Fabrezi and Alberch, 1996; Fabrezi and Barg, 2001). The condition of DC 4 + 5 of some specimens of

Myobatrachoidea available to us (e.g., *Uperoleia rugosa*, *U. fusca*, *U. russelli*, *Pseudophryne semimarmorata*, *Crinia signifera*, and *Myxophyes fasciolatus*) suggests that a third element might be involved in the formation of DC 4 + 5 at least in some taxa. *C. gayi* differs from *T. venustus* in the number of independent chondral nuclei involved in the formation of the Element Y. In *T. venustus*, three elements located in different spacial planes are visible, whereas only two occur in the earliest stage of *C. gayi* examined. Given that three cartilaginous condensations form Element Y in many neobatrachian anurans (Fabrezi and Barg 2001), we think probable that *C. gayi* might possess three condensations in an earlier developmental stage than was available to us. Carpal elements DC 2, DC 3, and pp1 originate from a single chondrification center in *T. venustus* and in *C. gayi*, as described for other anuran species (Fabrezi and Alberch, 1996; Fabrezi and Barg, 2001). The adult carpal morphologies of *C. gayi* and *T. venustus* are identical and result from a similar developmental pattern. This is important because identical adult carpal morphologies can be produced by different developmental pathways (Fabrezi, 1992; Fabrezi and Barg, 2001).

The anuran pelvic girdle differs from those of other tetrapods by having anteriorly projecting elongate ilial shafts that terminate ventral to the sacral diapophyses. Few studies have addressed the early development of this structure in anurans. In his classic work, Green (1931) studied histological sections of a complete developmental series of *Rana temporaria* and concluded that the puboischiadic and iliac portions of each half of the girdle arise from two different cartilaginous centers. According to Green, each ilium originates at the ilial shaft region, grows backward, and merges with the corresponding puboischiadic portion at the level of the posterior notch; this notch has been interpreted as the evidence of the inferred fusion. The presence of two cartilaginous anlage for each half of the pelvic girdle was confirmed by Ročková and Roček (2005), who considered the development of the pelvic girdle in various anuran species (*Xenopus laevis*, *Discoglossus pictus*, *Bombina variegata*, *B. bombina*, *Pelobates fuscus*, *Bufo bufo*, and *Rana dalmatina*). Recently, a detailed histological work by Pomikal et al. (2011) demonstrated the origin of the pelvic girdle from a single precartilaginous plate from which both puboischiadic and iliac portions arise. The latter authors indicated that there are no evident signs of tripartition; however, they did not specify the number of chondrification centers that condense within the procartilaginous plate. Our observations of the developmental series of *C. gayi* support the origin of a single cartilaginous plate on each side of the vertebral axis from which the pelvic girdle arises, contrary to Green (1931) and Ročková and Roček (2005). The semicircular morphology of the pelvic plate from which the ilial shaft subsequently develops and the presence of a posterior notch before the development of the ilial shaft argue against the findings of the referred studies. The ossification of the ventral portion of the puboisquiadic plate of *C. gayi*, which occurs in old individuals, is produced by the expansion of the ischium and ilium over the cartilage and not by an independent center of ossification.

The transitional existence of a DT 4 imbedded in the mediodistal cartilaginous end of the fibulare is an interesting feature of *C. gayi*. DT 4 can be identified in the earliest ontogenetic stages of the series (i.e., Stages 34–36), but it is not visible as a distinct chondrification thereafter; instead, it is indistinguishable from the cartilaginous end of the fibulare. This chondrification has been reported for *A. truei*, which has DTs 1–5 in Stage 39; by Stage 42, DTs 4 and 5 are fused to the distal end of the fibulare (Fabrezi, 1993).

In the course of this study, it became evident that the lack of osteological and developmental information on Australobatrachian prevents meaningful comparisons and interpretation of results. In addition, it was also manifest the enormous osteological diversity of this clade that radiated mainly in the Australian continent, although the paleontological evidence (e.g., Muzzopappa and Báez 2009) indicates an ancient and putative Gondwanan origin. We hope that the information provided here will seed future research on the evolution of this interesting, but enigmatic anuran lineage.

ACKNOWLEDGMENTS

Most of this research was carried out at the Departamento de Geología, Facultad de Ciencias Exactas y Naturales, Universidad de Buenos Aires, and at the Museo Argentino de Ciencias Naturales "Bernardino Rivadavia." The authors thank Santiago Reuil for his help in fieldwork and with many technical matters. Francisco Firpo, Boris Blotto, and Julián Faivovich provided advice about collecting, preserving, and clearing and staining techniques, and Agustín Scanferla helped with skeletonization techniques. The authors also acknowledge the contribution of Rafe Brown and Matt Buhler (University of Kansas) for access to the specimens under their care. Several aspects of this manuscript were enriched after beeing discussed with researchers at the División Herpetología, Museo Argentino de Ciencias Naturales "Bernardino Rivadavia" J. Sebastián Barrionuevo, Laura Nicoli, Boris Blotto, Martín Pereyra, and Julián Faivovich. The authors also thank Linda Trueb and an anonymous reviewer for critical comments and suggestions on the manuscript. Thanks are exteded to Pamela Biskupovic and Carola Mieville for providing lodging during the fieldwork in Chile.

LITERATURE CITED

Alcalde L. 2007. Desarrollo del esqueleto larvario y musculatura asociada en el género Batrachyla Bell 1843 (Anura: Neobatrachia) y sus relaciones filogenéticas interespecíficas [dissertation]. La Plata: Universidad de La Plata. 314 p.

Andersson LG. 1916. Results of Dr. E. Mjöbergs Swedish scientific expeditions to Australia, 1910–13. Batrachians from Queensland. Kungl Svenska Vetenskapsakad Handl 52:1–20.

Anstis M. 2013. Tadpoles and Frogs of Australia. Sydney: New Holland Press. 831 p.

Baleeva NV. 2001. Formation of the scapular part of the pectoral girdle in anuran larvae. Russ J Herpetol 8:195–204.

Baleeva NV. 2009. Formation of the coracoid region of the anuran pectoral girdle. Russ J Herpetol 16:41–50.

Banbury B, Maglia AM. 2006. Skeletal development of the Mexican spadefoot, *Spea multiplicata* (Anura: Pelobatidae). J Morphol 267:803–821.

Barrionuevo JS. 2013. Osteology and postmetamorphic development of *Telmatobius oxycephalus* (Anura: Telmatobiidae) with an analysis of skeletal variation in the genus. J Morphol 274: 73–96.

Barrionuevo JS, Baldo D. 2009. A new species of *Telmatobius* (Anura, Ceratophryidae) from Northern Jujuy Province, Argentina. Zootaxa 2030:1–20.

Bolkay SJ. 1919. Osnove uporedne osteologije anurskih batrahija sa dodatkom o porijeklu Anura i sa skicom naravnoga sistema istih. Glasn Zemaljsk Muz Bosni Hercegovini 1919: 277–353.

Boulenger GA. 1888. Descriptions of two new Australian frogs. Ann Mag Nat Hist Ser 6 2:142–143.

Castanet J, Francillon-Vieillot H, de Ricqlés A, Zylberberg L. 2003. The skeletal histology of the Amphibia. In: Heatwole H, Davies M, editors. Amphibian Biology. Chipping Norton: Surrey Beatty and Sons. pp 1598–1683.

Cei JM. 1962. Batracios de Chile. Santiago de Chile: Ediciones de la Universidad de Chile. 128 p.

Davies M. 1984. Osteology of the myobatrachine frog *Arenophryne rotunda* Tyler (Anura: Leptodactylidae) and comparisons with other myobatrachine genera. Aust J Zool 32:789–802.

Davies M. 1989. Ontogeny of bone and the role of heterochrony in the Myobatrachine genera *Uperoleia*, *Crinia* and *Pseudophryne* (Anura: Leptodactylidae: Myobatrachinae). J Morphol 200:269–300.

Davies M, Burton TC. 1982. Osteology and myology of the gastric brooding frog *Rheobatrachus silus* Liem (Anura: Leptodactylidae). Aust J Zool 30:503–521.

Davies M, Littlejohn MJ. 1986. Frogs of the genus *Uperoleia* Gray (Anura: Leptodactylidae) in South-Eastern Australia. Trans R Soc S Aust 110:111–143.

Davies M, McDonald KR. 1985. A redefinition of *Uperoleia rugosa* (Andersson) (Anura: Leptodactylidae). Trans R Soc S Aust 109:37–42.

Davies M, Roberts JD. 1985. A new speces of *Uperoleia* (Anura: Leptodactylidae) from the Pilbara Region, Western Australia. Trans R Soc S Aust 109:103–108.

Davies M, McDonald KR, Corben CJ. 1986. The genus *Uperoleia* (Anura: Leptodactylidae) in Queensland, Australia. Proc R Soc Victoria 98:147–188.

Davies M, Watson GF, McDonald KR, Trenerry MP, Werren G. 1993. A new species of *Uperoleia* (Anura: Leptodactylidae: Myobatrachinae) from Northeastern Australia. Mem Queensl Mus 33:167–174.

Díaz NF, Valencia J. 1985. Larval morphology and phenetic relationships of the Chilean *Alsodes*, *Telmatobius*, *Caudiverbera* and *Insuetophrynus* (Anura: Leptodactylidae). Copeia 1985:175–181.

Donnellan S, Mahony M, Davies M. 1990. A new species of *Mixophyes* (Anura: Leptodactylidae) and first record of the genus in New Guinea. Herpetologica 46:266–274.

Duellman WE, Trueb L. 1994. Biology of Amphibians. Baltimore: Johns Hopkins University Press. 670 p.

Duméril A-M, Bibron G. 1841. Erpétologie génerale du Histoire Naturelle complète des Reptiles. Paris: Librairie encyclopédique de Roret. 793 p.

Fabrezi M. 1992. El carpo de los anuros. Alytes 10:1–29.

Fabrezi M. 1993. The anuran tarsus. Alytes 11:47–63.

Fabrezi M, Alberch P. 1996. The carpal elements of anurans. Herpetologica 52:188–204.

Fabrezi M, Barg M. 2001. Patterns of carpal development among anuran amphibians. J Morphol 249:210–220.

Formas RJ, Núñez JJ, Brieva LM. 2001. Osteología, taxonomía y relaciones filogenéticas de las ranas del género *Telmatobufo* (Leptodactylidae). Rev Chil Hist Nat 74:365–387.

Frost DR. 2015. Amphibian Species of the World: an Online Reference. Version 6.0: American Museum of Natural History: New York, USA. Available at: http://research.amnh.org/herpetology/amphibia/index.html.

Frost DR, Grant T, Faivovich J, Bain RH, Hass A, Haddad CFB, De Sá RO, Channing A, Wilkinson M, Donnellan S, Raxworthy CJ, Campbell JA, Blotto BL, Molder P, Drewes RC, Nussbaum RA, Lynch JD, Green D, Wheeler W. 2006. The amphibian tree of life. Bull Am Mus Nat Hist 297:1–370.

Gaupp E. 1896. Eckers und Wiedersheim Anatomie des Frosches. Abt. 1. Lehre vom Skelet und vom Muskelsystem. Braunschweig: Druck und Verlag von Friederich Vieweg und Sohn. 229 p.

Girard C. 1853. Descriptions of new species of reptiles, collected by the U.S. Exploring Expedition, under the command of Capt. Charles Wilkes, U.S.N. Second part-including the species of batrachians, exotic to North America. Proc Acad Nat Sci Philadelphia 6:420–424.

Gosner KL. 1960. A simplified table for staging anuran embryos and larvae with notes on identification. Herpetologica 16:183–190.

Gradwell N. 1975. Experiments on oral suction and gill breathing in five species of Australian tadpole (Anura: Hylidae and Leptodactylidae). J Zool 177:81–98.

Gray JE. 1841. Description of some new species and four new genera of reptiles from western Australia, discovered by John Gould, Esq. Ann Mag Nat Hist Ser 1 7:86–91.

Gray JE. 1842. Description of some hitherto unrecorded species of Australian reptiles and batrachians. Zool Misc 2:51–57.

Green TL. 1931. On the pelvis of the Anura: A study in adaptation and recapitulation. Proc Zool Soc Lond 1931:1259–1290.

Griffiths I. 1959. The phylogenetic status of the Sooglossinae. Ann Mag Nat Hist Ser 13 2:626–640.

Günther ACLG. 1858a. Catalogue of the Batrachia salientia in the Collection of the British Museum. By Dr. Albert Günther. London: Printed by order of the Trustees. 8 p.

Günther ACLG. 1858b. Neue Batrachier in der Sammlung des britischen Museums. Arch Naturgesch 24:319–328.

Günther ACLG. 1863. On new species of batrachians from Australia. Ann Mag Nat Hist Ser 3 11:26–28.

Günther ACLG. 1864. Third contribution to our knowledge of batrachians from Australia. Proc Zool Soc Lond 1864:46–49.

Haas A. 2003. Phylogeny of frogs as inferred from primarily larval characters (Amphibia: Anura). Cladistics 19:23–89.

Hall JA, Larsen JHJ. 1998. Postembryonic ontogeny of the spadefoot toad, *Scaphiopus intermontanus* (Anura: Pelobatidae): skeletal morphology. J Morphol 238:179–244.

Handrigan GR, Wassersug RJ. 2007 The metamorphic fate of supernumerary caudal vertebrae in South Asian litter frogs (Anura: Megophryidae). J Anat 211:271–279.

Handrigan GR, Haas A, Wassersug RJ. 2007. Bony-tailed tadpoles: The development of supernumerary caudal vertebrae in larval megophryids (Anura). Evol Dev 9:190–202.

Harrison L. 1927. Notes on some Western Australian frogs, with descriptions of new species. Rec Aust Mus 15:277–287.

Havelková P, Roček Z. 2006. Transformation of the pectoral girdle in the evolutionary origin of frogs: insights from the primitive anuran *Discoglossus*. J Anat 209:1–11.

Hewitt J. 1913. Description of *Heleophryne natalensis*, a new batrachian from Natal; and notes on several South African batrachians and reptiles. Ann Natal Mus 2:475–484.

Heyer WR, Liem DSS. 1976. Analysis of the intergeneric relationships of the Australian frog family Myobatrachidae. Smithson Contrib Zool 233:1–29.
Jenkins FA, Shubin NH. 1998. *Prosalirus bitis* and the anuran caudopelvic mechanism. J Vert Paleontol 18:495–510.
Jorquera B, Izquierdo L. 1964. Tabla de desarrollo normal de Calyptocephalella gayi (rana chilena). Biologica, Santiago 36: 43–53.
Jorquera B, Pugin E. 1975. Organogénesis de la Rana Chilena (*Calyptocephalella caudiverbera*) (Amphibia, Leptodactylidae). Publ Oc Mus Nac Hist Nat Chile 20:3–29.
Keferstein W. 1868. Über die Batrachier Australiens. Arch Naturgesch 34:252–290.
Krieg H. 1924. Biologische reisestudien in Südamerika- II *Rhinoderma* und Calyptocephalus. Z Morph Ökol Tiere 3:150–168.
Lavilla EO. 1988. Lower Telmatobiinae (Anura: Leptodactylidae): generic diagnoses based on larval characters. Univ Kansas Mus Nat Hist Occ Pap 124:1–19.
Littlejohn MJ, Roberts JD, Watson GF, Davies M. 1993. Family Myobatrachidae. In: Glasby CG, Ross GJB, Beesley PL, editors. Fauna of Australia Volume 2A Amphibia and Reptilia. Australia: Australian Government Publishing Service. pp 1–46.
Lötters S, Reichle S, Faivovich J, Bain RH. 2005. The stream-dwelling tadpole of *Hyloscirtus charazani* (Anura: Hylidae) from Andean Bolivia. Stud Neotrop Fauna Environ 40:181–184.
Loveridge A. 1933. A new genus and three new species of crinine frogs from Australia. Occas Pap Boston Soc Nat Hist 8: 89–94.
Lucas AHS. 1892. Note on the distribution of Victorian batrachians, with descriptions of two new species. Proc R Soc Victoria 4:61–64.
Lynch JD. 1971. Evolutionary Relationships, Osteology, and Zoogeography of Leptodactyloid Frogs. Lawrence: University of Kansas. 238 p.
Lynch JD. 1973. The transition form archaic to advanced frogs. In: Vial J, editor. Evolutionary Biology of the Anurans Contemporary Research on Major Problems. Columbia: University of Missouri Press. pp 133–182.
Lynch JD. 1978. A re-assessment of the Telmatobiine leptodactylid frogs of Patagonia. Univ Kansas Mus Nat Hist Occ Pap 72:1–57.
Mahony M, Tyler MJ, Davies M. 1984. A new species of the genus *Rheobatrachus* (Anura: Leptodactylidae) from Queensland. Trans R Soc S Aust 108:155–162.
Main AR. 1957. Studies in Australian Amphibia. I. The genus *Crinia* Tschudi in South-Western Australia and some species from South-Eastern Australia. Aust J Zool 5:30–55.
Marelli CA. 1927. Una interesante anomalía por sacralización coxígea del batracio *Calyptocephalus Gayi* D. y B. Rev Chil Hist Nat 31:237–240.
Martin AA, Tyler MJ, Davies M. 1980. A new species of *Ranidella* (Anura: Leptodactylidae) from northwestern Australia. Copeia 1980:93–99.
Mookerjee HK. 1931. On the development of the vertebral column of Anura. Philos Trans R Soc Lond 219:165–196.
Mookerjee HK, Das K. 1939. Further investigation on the development of the vertebral column in Salientia (Anura). J Morphol 3:167–209.
Moore JA. 1958. A new genus and species of leptodactylid frog from Australia. Am Mus Novit 1919:1–7.
Moore JA. 1961. Frogs of eastern New South Wales. Bull Am Mus Nat Hist 121:149–386.
Moreno A, Crovari D, Miranda D, Oróstegui C, Salibián A. 1978. Histología de la piel de *Calyptocephalella caudiverbera*. Not Mens Mus Nac Hist Nat Chile 22:3–11.
Muzzopappa P, Báez AM. 2009. Systematic status of the mid-Tertiary neobatrachian frog *Calyptocephalella canqueli* from Patagonia (Argentina), with comments on the evolution of the genus. Ameghiniana 46:113–125.
Nieden F. 1923. Amphibia Anura I. Das Tierreich 46:xxxii+584 p.
Parker HW. 1940. The Australasian frogs of the family Leptodactylidae. Novit Zool 42:1–106.
Parker WK. 1881. On the structure and development of the skull in the Batrachia. Part III. Philos Trans R Soc Lond 172: 1–266.
Peters WCH. 1863. Eine Übersicht der von Hrn. Richard Schomburgk an das zoologische Museum eingesandten Amphibien, aus Buchsfelde bei Adelaide in Südaustralien. Monatsber Preuss Akad Wiss Berlin 1863:228–236.
Philippi RA. 1899. Sobre las serpientes de Chile. An Univ Chile 104:715–725.
Pomikal C, Blumer R, Streicher J. 2011. Four-Dimensional analysis of early pelvic girdle development in *Rana temporaria*. J Morphol 272:287–301.
Procter JB. 1921. On the variation of the scapula in the batrachian groups Aglossa and Arcifera. Proc Zool Soc Lond 91: 197–214.
Pugener LA. 2002. The Vertebral Column and Spinal Nerves of Anurans [dissertation]. Lawrence: University of Kansas. 480 p.
Púgener LA, Maglia AM. 1997. Osteology and skeletal development of *Discoglossus sardus* (Anura: Discoglossidae). J Morphol 233:267–286.
Pugener LA, Maglia AM. 2009. Skeletal morphogenesis of the vertebral column of the miniature hylid frog *Acris crepitans*, with comments on anomalies. J Morphol 270:52–69.
Pyron RA, Wiens JJ. 2011. A large-scale phylogeny of Amphibia including over 2800 species, and a revised classification of extant frogs, salamanders, and caecilians. Mol Phylogenet Evol 61:543–583.
Rabanal F, Núñez J. 2008. Anfibios de los bosques templados de Chile. Valdivia: Universidad Austral de Chile y Extensión UACh. 202 p.
Reig OA. 1960. Las relaciones genéricas del anuro chileno *Calyptocephalella gayi* (Dum. & Bibr.). Actas y Trabajos del Primer Congreso Sudamericano de Zoología 4. La Plata. pp 113–131.
Reinbach W. 1939. Untersuchungen über die Entwicklung des Kopfskeletts von *Calyptocephalus gayi*. Jen Zeit Natur 72: 211–362.
Roček Z. 2003. Larval development and evolutionary origin of the anuran skull. In: Heatwole H, Davies M, editors. Amphibian Biology – Osteology. Chipping Norton: Surrey Beaty and Soons. pp 1877–1999.
Ročková H, Roček Z. 2005. Development of the pelvis and posterior part of the vertebral column in the Anura. J Anat 206: 17–35.
Sánchez DA. 2010. Larval development and synapomorphies for species groups of *Hyloscirtus* Peters, 1882 (Anura: Hylidae: Cophomantini). Copeia 2010:351–363.
Sanchiz BJ, Tejedo M, Sánchez-Herráiz MJ. 2002. Osteological differentiation among Iberian *Pelodytes* (Anura, Pelodytidae). Graellsia 58:35–68.
San Mauro D, Vences M, Alcobendas M, Zardoya R, Meyer A. 2005. Initial diversification of living amphibians predated the breakup of Pangea. Am Nat 165:590–599.
Schmidt KL. 1952. A new leptodactylid frog from Chile. Fieldiana Zool 34:11–15.
Sedra SN, Moursi AA. 1958. The ontogenesis of the vertebral column of Bufo regularis Reuss Cesk Morf VI:7–32.
Simmons JE. 1986 A method of preparation of anuran osteological material. 1986. In: Waddington J, Rudkin DM, editors. Proceedings of the 1985 Workshop on Care and Maintenance of Natural History Collections. Toronto: R Ont Mus Life Sci Misc Publ. pp 37–39.
Spencer B. 1901. Two new species of frogs from Victoria. Proc R Soc Victoria 13:176–178.
Stephenson NG. 1951. Observations on the development of the amphicoelus frogs, *Leiopelma* and *Ascaphus*. J Linn Soc Lond Zool 42:18–28.
Stephenson NG. 1965. Heterochronous changes among Australian leptodactylid frogs. Proc Zool Soc Lond 144:339–350.

Talavera RR. 1990. Evolución de pelobátidos y pelodítidos (Amphibia, Anura): Morfología y desarrollo del sistema esquelético [dissertation]. Madrid: Universidad Complutense. 282 p.

Taylor WR, van Dyke G. 1985. Revised procedure for staining and clearing small fishes and other vertebrates for bone and cartilage study. Cybium 9:107–111.

Tyler MJ. 1972. New genus for the Australian leptodactylid frog *Crinia darlingtoni*. Zool Meded 47:193–201.

Tyler MJ. 1976a. Comparative osteology of the pelvic girdle of Australian frogs and description of a new fossil genus. Trans R Soc S Aust 100:3–14.

Tyler MJ. 1976b. A new genus and two new species of leptodactylid frogs from Western Australia. Rec West Aust Mus 4:45–52.

Tyler MJ, Davies M. 1980. Systematic status of *Kankanophryne* Heyer & Liem (Anura: Leptodactylidae). Trans R Soc S Aust 104:17–20.

Tyler MJ, Davies M, Martin AA. 1981. New and rediscovered species of frogs from the Derby Broome Area of Western Australia. Rec West Aust Mus 9:147–172.

Tyler MJ, Davies M, Watson GF. 1987. Frogs of the Gibb River Road, Kimberley Division, Western Australia. Rec West Aust Mus 13:541–552.

Van Der Meijden A, Boistel R, Gerlach J, Ohler A, Vences M, Meyer A. 2007. Molecular phylogenetic evidence for paraphyly of the genus *Sooglossus*, with the description of a new genus of Seychellean frogs. Biol J Linn Soc Lond 91:347–359.

Wiens JJ. 1989. Ontogeny of the skeleton of *Spea bombifrons* (Anura: Pelobatidae). J Morphol 202:29–51.

Wild ER. 1997. Description of the adult skeleton and developmental osteology of the hyperossified Horned Frog, *Ceratophrys cornuta* (Anura: Leptodactylidae). J Morphol 232:169–206.

Wild ER. 1999. Description of the chondrocranium and osteogenesis of the Chacoan burrowing frog, *Chacophrys pierotti* (Anura: Leptodactylidae). J Morphol 242:229–246.

Witten PE, Huysseune A. 2007. Mechanisms of chondrogenesis and osteogenesis in fins. In: BK H, editor. Fins into Limbs: Evolution, Development, and Transformation. Chicago: The University of Chicago Press. pp 79–92.

Wu S-H. 1994. Phylogenetic relationships, higher classification, and historical biogeography of the microhyloid frogs (Lissamphibia: Anura: Brevicipitidae and Microhylidae) [dissertation]. Ann Arbor: The University of Michigan. 284 p.

Zweifel RG. 1972. A review of the frog genus *Lechriodus* (Leptodactylidae) of New Guinea and Australia. Am Mus Novit 2507:1–41.